

Contract No:

This document was prepared in conjunction with work accomplished under Contract No. DE-AC09-08SR22470 with the U.S. Department of Energy (DOE) Office of Environmental Management (EM).

Disclaimer:

This work was prepared under an agreement with and funded by the U.S. Government. Neither the U. S. Government or its employees, nor any of its contractors, subcontractors or their employees, makes any express or implied:

- 1) warranty or assumes any legal liability for the accuracy, completeness, or for the use or results of such use of any information, product, or process disclosed; or
- 2) representation that such use or results of such use would not infringe privately owned rights; or
- 3) endorsement or recommendation of any specifically identified commercial product, process, or service.

Any views and opinions of authors expressed in this work do not necessarily state or reflect those of the United States Government, or its contractors, or subcontractors.

We put science to work.™



**Savannah River
National Laboratory™**

OPERATED BY SAVANNAH RIVER NUCLEAR SOLUTIONS

A U.S. DEPARTMENT OF ENERGY NATIONAL LABORATORY • SAVANNAH RIVER SITE • AIKEN, SC

Determining the Release of Radionuclides from Tank 18F Waste Residual Solids: FY2016 Report

William D. King

David T. Hobbs

August 2016

SRNL-STI-2016-00432, Revision 0

SRNL.DOE.GOV

DISCLAIMER

This work was prepared under an agreement with and funded by the U.S. Government. Neither the U.S. Government or its employees, nor any of its contractors, subcontractors or their employees, makes any express or implied:

1. warranty or assumes any legal liability for the accuracy, completeness, or for the use or results of such use of any information, product, or process disclosed; or
2. representation that such use or results of such use would not infringe privately owned rights; or
3. endorsement or recommendation of any specifically identified commercial product, process, or service.

Any views and opinions of authors expressed in this work do not necessarily state or reflect those of the United States Government, or its contractors, or subcontractors.

Printed in the United States of America

**Prepared for
U.S. Department of Energy**

Keywords: *groundwater, infiltration water, grout pore water, high level waste, tank closure, pH, E_h , oxidation-reduction potential*

Retention: *Permanent*

Determining the Release of Radionuclides from Tank 18F Waste Residual Solids: FY2016 Report

William D. King
David T. Hobbs

August 2016

Prepared for the U.S. Department of Energy under contract number DE-AC09-08SR22470.

REVIEWS AND APPROVALS

AUTHORS:

W. D. King, Advanced Characterization and Process Technology Date

D. T. Hobbs, Separations and Actinide Science, Date

TECHNICAL REVIEW:

M. S. Hay, Advanced Characterization and Process Technology, Reviewed per E7 2.60 Date

APPROVAL:

B. J. Wiedenman, Manager Date
Advanced Characterization and Process Technology

D. E. Dooley, Director Date
Environmental & Chemical Process Technology Research Programs

K. H. Rosenberger Date
Waste Disposal Authority

ACKNOWLEDGEMENTS

Joshua Perry, Gary Hall, Ron Blessing, and Victor Skeens worked closely with the authors to design and prepare the test equipment. The customized equipment design would not have been possible without the creativity and unique capabilities of these individuals. Remote sample and equipment handling in the SRNL shielded cells facility were conducted by Rita Sullivan and Jeff Mixon. Rita and Jeff worked tirelessly to accomplish the test objectives and conducted numerous unexpected and challenging equipment manipulations to complete the testing. Their positive attitudes and work ethic resulted in an enjoyable and productive work environment. In addition, support from numerous other personnel in the shielded cells was needed periodically. Mona Blume also provided periodic support for work conducted outside of the shielded cells and provided some needed supplies. Chris Martino and Cap Nguyen provided the equipment photographs. Miles Denham provided insight regarding the Performance Assessment modeling which influenced the testing approach and the data analysis. We also acknowledge support from the SRNL Analytical Development (AD) section. Specifically, David Diprete and Mark Jones provided the metal concentrations for samples obtained from the pore water leaching studies.

EXECUTIVE SUMMARY

Pore water leaching studies were conducted on actual Savannah River Site (SRS) Tank 18F residual waste solids to support Liquid Waste tank closure efforts. A test methodology was developed during previous simulant testing to produce slurries of tank residual solids and grout-representative solids in grout pore water solutions (based on SRS groundwater compositions) with pH and E_h values expected during the aging of the closed waste tank. The target conditions are provided below where the initial pore water has a reducing potential and a relatively high pH (Reducing Region II). The pore water is expected to become increasingly oxidizing with time (Oxidizing Region II) and during the latter stages of aging (Oxidizing Region III) the pH is expected to decrease. For the reducing case, tests were conducted with both unwashed and washed Tank 18F residual solids. For the oxidizing cases (Oxidizing Regions II and III), all samples were washed with simulated grout pore water solutions prior to testing, since it is expected that these conditions will occur after considerable pore water solution has passed through the system. For the reducing case, separate tests were conducted with representative ground grout solids and with calcium carbonate reagent, which is the grout phase believed to be controlling the pH. Ferrous sulfide (FeS) solids were also added to the reducing samples to lower the slurry E_h value. Calcium carbonate solids were used as the grout-representative solid phase for each of the oxidizing cases. Air purge-gas with and without CO_2 removed was transferred through the oxidizing test samples and nitrogen purge-gas was transferred through the reducing test samples during leach testing. The target pH values were achieved to within 0.5 pH units for all samples. Leaching studies were conducted over an E_h range of approximately 0.7 V. However, the highest and lowest E_h values achieved of $\sim+0.5$ V and ~-0.2 V were significantly less positive and less negative, respectively, than the target values. Achievement of more positive and more negative E_h values is believed to require the addition of non-representative oxidants and reductants, respectively.

Soluble metal concentrations determined for slurry sub-samples collected during Tank 18F residual solids leaching studies (shown below) followed the general trends predicted for plutonium and uranium oxide phases, and were generally consistent with simulant test results. The highest plutonium and uranium concentrations were observed for Oxidizing Region III (test sample C) and the lowest concentrations were observed for Reducing Region II in the presence of grout solids (test sample F). The highest technetium concentrations measured during leaching studies were observed for the oxidizing cases (Oxidizing Regions II and III, test samples A, B, and C) and the lowest concentrations (non-detectable amounts) were observed for the reducing cases (test samples E and F). The highest neptunium concentrations were observed for Oxidizing Region III (test sample C) and similarly low and non-detectable concentrations were observed for both the Reducing Region II cases (test samples E and F) and one Oxidizing Region II case (test sample A). Comparing the solubilities of each of the metals analyzed, uranium is much more soluble than all of the other metals analyzed in the leach studies with the maximum observed concentration near $4E-4$ M for U, while the maximum concentrations of each of the other metals were $<5E-8$ M. The maximum metal concentrations observed during leach testing for plutonium, neptunium, and technetium were all below the predicted values assuming equilibrium with dissolved oxygen. However, uranium concentrations in the leachate solutions exceeded predictions.

After leach test completion, selected residual sample wash solutions were analyzed to determine the metal losses to the wash and it was discovered that concentrations in the wash solutions under oxidizing conditions were higher than were observed for any leach test sample. The measured concentrations for the ORII-A and ORIII-C wash solutions are provided in the table below. The concentrations of plutonium, uranium, and neptunium also significantly exceeded the predicted values assuming equilibrium with dissolved oxygen. Mass balance calculations based on these concentrations indicate that all of the uranium in the ORIII-C and probably in the ORIII-D sample dissolved in the wash prior to leach testing. Based on this information, the uranium concentrations reported for the leachate samples are not

highly meaningful. Less than 15% of each of the other metals (excluding uranium) dissolved in the wash. These results indicate that it is possible to exceed the observed leachate concentrations during initial pore water contacts. Higher concentrations in the washes indicate that some portion of the metals may exist as more soluble or more kinetically accessible phases. Despite these results, the metal concentrations observed in the leach testing are still believed to conservatively represent the levels that would be achieved during the majority of the tank aging periods of interest, although these concentrations could be exceeded upon initial contact with oxidizing solutions.

Evaluation of blank samples collected during testing indicate that the leachate metal concentrations analyzed are representative of Tank 18F residual waste component dissolution under the conditions of interest rather than resulting from contamination from the shielded cells environment. This result and the general agreement between the simulant and actual waste testing confirm that the test methodology developed and the equipment designed were successfully utilized to evaluate the metal solubilities and leaching characteristics of Tank 18F residual solids under the conditions of interest. This approach should be suitable for leach testing of other tank residual materials as well.

Target Pore Water Conditions.

PA Target Condition	E _h (mV)	pH
Reduced Region II (RRII)	-470	11.1
Oxidized Region II (ORII)	+560	11.1
Oxidized Region III (ORIII)	+680	9.2

Measured pH, E_h, and Metal Concentrations for Each Pore Water Test Condition Using Actual Tank 18F Residual Solids.

Test Condition	Sample ID	Additives	Atmosphere	E _h ^a (mV)	pH ^a	Pu ^a (M)	U ^{a,d} (M)	Tc ^a (M)	Np ^b (M)
RRII	E	Ca(OH) ₂ , CaCO ₃ , FeS	continuous N ₂ purge	-208	10.9	2E-9	2E-6	<6E-10	<2E-10
RRII	F	CFS ^c , FeS	continuous N ₂ purge	-196	11.4	7E-11	2E-6	<6E-10	<2E-10
ORII	A	Ca(OH) ₂ , CaCO ₃	continuous air purge	+351	11.2	4E-10	4E-6	1E-8	<2E-10
ORII	B	Ca(OH) ₂ , CaCO ₃	continuous air purge	+328	10.8	6E-9	2E-5	1E-8	3E-10
ORIII	C	CaCO ₃	continuous air or CO ₂ -stripped air purge	+520	9.4	1E-8	4E-4	1E-8	4E-9
ORIII	D	CaCO ₃	continuous air or CO ₂ -stripped air purge	+493	9.3	6E-9	7E-5	6E-9	1E-9

^a average data from final 4 weeks

^b average data from final 2-3 weeks

^c CFS = cement, flyash, and slag grout solids

^d due to nearly complete U dissolution observed during washing these leachate concentrations are likely well below solubility limits

Metal Concentrations Observed for ORII-A and ORIII-C Wash Solutions.

	Pu (M)	U (M)	Np (M)	Tc (M)
ORII-A	4.0E-08	3.2E-04	1.3E-09	1.0E-08
ORIII-C	3.0E-07	4.6E-03	2.9E-08	9.4E-09

TABLE OF CONTENTS

LIST OF TABLES	x
1.0 Introduction	1
2.0 Experimental	1
2.1 Preparation of Synthetic Infiltration Water	1
2.2 Preparation of Grout Pore Water Simulants from SIW	2
2.3 Tank 18F Residual Waste Solids	3
2.4 Equipment Design and Operation	4
2.5 Leaching Studies	9
2.6 Sample Analysis	11
2.7 Quality Assurance	11
3.0 Results and Discussion	12
4.0 Conclusions	34
5.0 Recommendations, Path Forward, and Future Work	35
6.0 References	36
Appendix A . SEM Analysis Results	37

LIST OF TABLES

Table 2-1. Synthetic Infiltration Water Concentrate Stock Solution Recipe.	2
Table 2-2. As-Prepared Elemental Composition of Synthetic Infiltration Water Simulant After Dilution. 2	
Table 2-3. Target Grout Pore Water Conditions.	2
Table 2-4. Summarized Tank 18F Sample FTF-1 Elemental Composition as Reported by Oji.	3
Table 2-5. Summarized Tank 18F Sample FTF-1 Radionuclide Composition as Reported by Oji.	4
Table 2-6. Test Sample and Reagent Masses and Solution Volumes.	11
Table 2-7. Test Sample Preparation and Sub-Sampling Timeline and Comments.	12
Table 2-8. Test Sample Wash Decant Volumes.	12
Table 3-1. Measured pH and E_h Data and Metal Concentrations for Each Pore Water Condition with Actual Tank 18F Residual Solids.	14
Table 3-2. Leaching Study Control Sample Analysis Results.	15
Table 3-3. Estimated Maximum Metal Losses to Tank 18F Residual Washes Prior to Leach Testing.	18
Table 3-4. Predicted Solubilities of Assumed Pu and U Phases.	23
Table 3-5. Measured pH, E_h , and Metal Concentrations for Each Pore Water Test Condition Using Actual Tank 18F Residual Solids.	24
Table 3-6. Predicted Solubilities of Assumed Tc and Np Phases.	26
Table 3-7. Additional Analysis Conducted on Week 7 Sub-samples.	27
Table 3-8. Americium Data for Week 3 Sub-samples.	28
Table 3-9. ORII-A and ORIII-C Wash Sample Analysis Results.	28
Table 3-10. Metal Losses to Tank 18F Residual Washes Prior to Leach Testing Calculated Based on Wash Analysis.	28
Table 3-11. Elemental Composition of Original Tank 18F Residual Solids and ORIII-C and RRII-E Leachate Samples at Test Conclusion.	29
Table 3-12. Elemental Weight Percentages Normalized to Aluminum for Original Tank 18F Residual Solids and ORIII-C and RRII-E Leachate Samples at Test Conclusion.	30

LIST OF FIGURES

Figure 2-1. Photograph of Testing Equipment Prior to Installation into the SRNL Shielded Cells.	5
Figure 2-2. Photograph of Leach Testing Sample Vessel.	6
Figure 2-3. Vessel and Plumbing Layout for SRNL Shielded Cells Testing.	7

Figure 2-4. Photograph of Initial Sub-Sampling System and Analysis Sample Vessels with Attached Vent Lines. 9

Figure 2-5. Photograph of Modified Sub-Sampling System..... 9

Figure 3-1. Photograph of Testing Equipment After Installation in the SRNL Shielded Cells and After Sample Addition/Preparation..... 15

Figure 3-2. Photograph of Test Vessels in the SRNL Shielded Cells at Test Conclusion..... 16

Figure 3-3. Slurry pH Data Collected During Tank 18F Residual Solids Leaching Studies. 16

Figure 3-4. Slurry E_h Data Collected During Tank 18F Residual Solids Leaching Studies. 17

Figure 3-5. Plutonium Concentrations Versus Time During Tank 18F Residual Solids Leaching Studies for Oxidizing Conditions. 17

Figure 3-6. Plutonium Concentrations Versus Time During Tank 18F Residual Solids Leaching Studies for Reducing Conditions. Note: Data labeled as -1 and -2 was collected prior to and after the final wash, respectively..... 18

Figure 3-7. Uranium Concentrations Versus Time During Tank 18F Residual Solids Leaching Studies for Oxidizing Conditions..... 21

Figure 3-8. Uranium Concentrations Versus Time During Tank 18F Residual Solids Leaching Studies for Reducing Conditions. 21

Figure 3-9. Technetium Concentrations Versus Time During Tank 18F Residual Solids Leaching Studies for Oxidizing Conditions. 22

Figure 3-10. Neptunium Concentrations versus Time during Tank 18F Residual Solids Leaching Studies for Oxidizing Conditions. 22

Figure 3-11. XRD Analysis Results for the Original, Archived Tank 18F Residual Solids. 25

Figure 3-12. XRD Analysis Results for the Tank 18F Residual Solids ORIII-C Leachate Sample at Test Conclusion. 30

Figure 3-13. XRD Analysis Results for the Tank 18F Residual Solids RRII-E Leachate Sample at Test Conclusion. 31

Figure 3-14. Volume-Based Particle Size Distribution for the Original Tank 18 Residual Solids in RRII Simulant..... 32

Figure 3-15. Volume-Based Particle Size Distribution for the ORIII-C Leachate Sample at Test Conclusion..... 32

Figure 3-16. Volume-Based Particle Size Distribution for the RRII-E Leachate Sample at Test Conclusion..... 33

Figure 3-17. Volume-Based Particle Size Distribution for the FeS Reagent in RRII Simulant. 33

Figure 3-18. Volume-Based Particle Size Distribution for the CaCO₃ Reagent in ORIII Simulant..... 34

LIST OF ABBREVIATIONS

AD	Analytical Development
APHA	Alpha Pulse Height Analysis
CFS	Cement, Flyash, and Slag grout solids
DOE	Department of Energy
EM	Environmental Management
GPHA	Gamma Pulse Height Analysis
FY	Fiscal Year
HLW	High Level Waste
ICP-ES	Inductively Coupled Plasma – Emission Spectroscopy
ICP-MS	Inductively Coupled Plasma – Mass Spectroscopy
IC	Ion Chromatography
ID	Inside Diameter
KAPL	Knolls Atomic Power Laboratory
LDPE	Low Density Polyethylene
OD	Outside Diameter
ORII	Oxidizing Region II
ORIII	Oxidizing Region III
ORP	Oxidation-Reduction Potential
PA	Performance Assessment
PSD	Particle Size Determination
PVDF	Poly Vinyl Difluoride
RRII	Reducing Region II
RPM	Rotations per Minute
SHE	Standard Hydrogen Electrode
SEM	Scanning Electron Microscopy
SIW	Synthetic Infiltration Water
SRNL	Savannah River National Laboratory
SRR	Savannah River Remediation
SRS	Savannah River Site
TTQAP	Task Technical and Quality Assurance Plan
XRD	X-ray Diffraction

1.0 Introduction

Current practice for closing High Level Waste (HLW) tanks at the Savannah River Site (SRS) involves removing waste to the maximum extent practical, disconnecting all transfer lines and penetrations into the tanks, and filling the internal volume of the tanks with grout (concrete). As of July 2016, Savannah River Remediation (SRR) has closed SRS Tanks 5, 6, 12, 16, 17, 18, 19, and 20. Performance Assessment (PA) modeling of the release of radionuclides from residual waste solids in these tanks into the environment over extended time periods indicated that uranium, plutonium, neptunium, and technetium are among the most likely risk drivers for environmental contamination.¹ The PA and supporting waste release modeling² indicated that plutonium release from SRS Tank 18F residuals (which contained relatively high Pu concentrations) was highest during the period identified as Oxidizing Region III (ORIII; predicted to occur after >2,120 pore volumes of grout pore water have passed through the system) when the system pore water has a pH of 9.2 and an E_h value of +680 mV (Oxidation Reduction Potential versus the Standard Hydrogen Electrode). At this stage, the dominant grout phase is expected to be calcite (CaCO_3). (Note: Grout pore water is defined as natural infiltrating groundwater exposed to the grout fill material and the residual waste solids layer within the closed tank environment. Furthermore, a pore volume represents the total volume of the pore voids within the grout fill material inside the closed tank.)

Waste release testing was requested to provide additional information regarding the residual waste solubility assumptions used in the SRS F- and H-Area Tank Farm PA Waste Release Models. The proposed testing is described generally in the SRS Liquid Waste Facilities PA Maintenance Program FY2015 Implementation Plan.³ This plan proposed that waste release experiments be performed with actual tank waste residuals after the completion of test method development using surrogate materials. SRR requested that the Savannah River National Laboratory (SRNL) design and perform such testing.⁴ In fiscal year (FY) 2014, a summary report on initial method development testing was issued with recommendations that additional testing be conducted with surrogates prior to actual waste testing.⁵ In FY2015, additional surrogate testing was conducted and a test methodology was developed as described in the associated summary report.⁶ The FY2015 summary report recommended that actual waste testing be conducted using the test methodologies developed. A Task Technical and Quality Assurance Plan (TTQAP) revision which included the requirements for actual waste testing was subsequently issued in October of 2015.⁷

Three theoretical periods and conditions occurring at different times following tank closure have been targeted for testing.² Reduced Region II (RRII) was predicted to occur initially following tank closure and to represent the conditions during the passage of the first portion (<520 pore volumes) of grout pore water through the closed tank system. Oxidizing Region II (ORII) was predicted to occur after RRII and to represent an intermediate condition (from >520 to <2,120 grout pore volumes). Oxidizing Region III (after >2,120 pore volumes) was the final target condition. Solution pH and E_h values have been predicted for each condition. This document provides results from FY2016 testing targeting these conditions using actual Tank 18F residual solids.

2.0 Experimental

2.1 Preparation of Synthetic Infiltration Water

A Synthetic Infiltration Water (SIW) concentrated stock solution was prepared from ultrapure water (Milli-Q) and the reagent grade chemicals shown in Table 2-1. The SIW stock solution used for FY2014 and FY2015 testing was also used for FY2016 testing. The SIW stock solution was diluted 1000:1 (1 mL SIW stock diluted into 1 L deionized water) prior to use for the preparation of grout pore water

formulations. The as-prepared elemental composition of the resulting SIW solution is provided in Table 2-2. The SIW was based on the average composition observed for groundwater from non-impacted wells within the SRS water table aquifer.⁴

Table 2-1. Synthetic Infiltration Water Concentrate Stock Solution Recipe.

Chemical Reagent	Concentration (g/L)
CaCl ₂ ·2H ₂ O	3.68
Na ₂ SO ₄	1.07
KCl	0.40
NaCl	2.65
MgCl ₂ ·6H ₂ O	5.51

Table 2-2. As-Prepared Elemental Composition of Synthetic Infiltration Water Simulant After Dilution.

Ion	Concentration (mg/L)
Na ⁺	1.39
K ⁺	0.21
Mg ²⁺	0.66
Ca ²⁺	1.00
Cl ⁻	5.51
SO ₄ ²⁻	0.73

2.2 Preparation of Grout Pore Water Simulants from SIW

The target pH and E_h values for three grout pore water solutions (based on the PA¹ and supporting modeling²) developed from the SIW and used for radionuclide release leaching studies are provided in Table 2-3.

Table 2-3. Target Grout Pore Water Conditions.

Target Condition	pH	E _h (mV)
Reduced Region II (RRII)	11.1	-470
Oxidized Region II (ORII)	11.1	+560
Oxidized Region III (ORIII)	9.2	+680

Grout pore water simulants were prepared for each condition in Table 2-3 as described below based on simulant modeling and recipe development previously conducted.⁶ RRII and ORII solutions were prepared from the diluted SIW by the addition of approximately 0.1 g CaCO₃/L and ≥0.05 g Ca(OH)₂/L to achieve a pH near 11 (reagent grade chemicals used in all cases). The resulting solution contained a trace of solids (presumably CaCO₃ solids based on modeling predictions). The RRII and ORII pore water simulants had the same chemical composition and differed only in the gaseous atmosphere ultimately

used to adjust the solution E_h values. ORIII simulant was prepared from the SIW by the addition of 0.1 g CaCO_3/L . This resulted in a solution containing trace amounts of (presumably) CaCO_3 solids with a pH near 10. Subsequent, brief (~15 minutes) purging of the solution with air resulted in the absorption of CO_2 and a reduction in the solution pH to near 9. All of the as-prepared simulants had solution E_h values near +500 mV. Purging the RRII simulant with nitrogen gas overnight resulted in a solution E_h value near -100 mV. Subsequent addition of reagent grade ferrous sulfide (FeS) solids while continuously purging the solution with inert gas resulted in solution E_h values near -200 mV (FeS not added in this study until test samples were prepared in the shielded cells facility). Previous testing and analysis revealed that these preparations result in elevated calcium concentrations ranging from 7-28 mg/L relative to the target composition of 1 mg Ca/L for the as-prepared simulant.⁶

The final step in the preparation of grout pore water simulants and test samples was the transfer of additional calcium carbonate, actual grout solids, or FeS (reducing samples only) to the solution in the shielded cells environment prior to actual waste leach testing. Calcium carbonate reagent was utilized as a grout-representative phase in all ORII and ORIII tests and in one RRII test to simplify the system and allow for better control of the solution pH and E_h . Cement, Fly Ash, and Slag (CFS) grout solids were utilized in the remaining RRII test. The CFS solids were initially prepared as a monolith representing the components of the grout used to fill SRS Tank 18F. The CFS solids recipe included 125 parts of Cement Type I/II, 210 parts of Slag Grade 100, and 363 parts of Fly Ash Class F. Sand was not added as a component of the monolith since both fly ash and slag contain significant quantities of silicon. Prior to contact with the SIW, the CFS monolith was broken into pieces which were then crushed and sieved through a 100 mesh sieve. The CFS powder was stored and transferred into the shielded cells in small vials containing no head space volume in order to minimize air exposure of the grout.

2.3 Tank 18F Residual Waste Solids

An archived sample of residual solids retrieved from the floor of SRS Tank 18F prior to tank closure was utilized for leach testing. The material was identified in the previous characterization report as Tank 18F Sample FTF-1.⁸ The sample composition is summarized in Tables 2-4 and 2-5 based on the detailed characterization reported.

Table 2-4. Summarized Tank 18F Sample FTF-1 Elemental Composition as Reported by Oji⁸.

Element	Wt. %
Al	11.0
Ca	2.9
Fe	9.8
Mg	3.8
Mn	1.0
Si	2.2
U	6.3

Table 2-5. Summarized Tank 18F Sample FTF-1 Radionuclide Composition as Reported by Oji⁸.

Radionuclide	μCi/g
Tc-99	2.7E-02
Th-229	1.9E-05
Th-230	1.4E-04
U-233	1.2E-03
U-234	2.0E-02
U-238	2.0E-02
Np-237	9.1E-03
Pu-238	5.7E+00
Pu-239	1.6E+01
Pu-240	3.6E+00
Pu-241	1.6E+01
Am-241	7.5E+00
Cm-244	1.2E-01

2.4 Equipment Design and Operation

Probes for the measurement of slurry pH and Oxidation-Reduction Potential (ORP) were installed in the shielded cells utilizing standard KAPL (Knolls Atomic Power Laboratory) plug penetrations through the front cell wall. Both pH and ORP data were measured with a dual channel Thermo Scientific™ Orion™ Star Series meter. Slurry pH data was collected during leach testing using a sealed, double-junction Oakton pH Electrode with an Epoxy body (Model WD-35805-01). The pH meter was calibrated prior to each use with pH 4, 7, and 10 standard buffer solutions. E_h data was collected using a Thermo Scientific 9179BN Low Maintenance ORP Triode with an Epoxy body. The E_h probes were checked using Thermo Scientific™ Oxidation-Reduction Potential (ORP) Standard 967901. The standard was checked once during each series of ORP sample measurements and all standard measurements ranged from +218 to +222 mV (E_h range: +418 to +422 mV). All reported sample E_h values are relative to the Standard Hydrogen Electrode (SHE). A standard correction of +200 mV was applied to all ORP data to convert the data to E_h format (Oxidation-Reduction Potential versus SHE), based on the manufacturer instructions and data obtained for the ORP standard. The electrode manuals indicate that the measured ORP values may vary by as much as ±60 mV.

A methodology was developed during testing for achieving consistent ORP measurements. Careful attention was given to the electrode behavior during sample measurements to ensure that accurate data was being collected. Under oxidizing conditions, a measurement time of 10 minutes was selected for probe stabilization and data recording. Under reducing conditions, it was found that long time periods (several hours) were often needed for measurement stabilization. Common practice for the reducing samples was to leave the electrode in one solution overnight to achieve a stable reading. Then the electrode was immediately transferred to the next sample requiring measurement under reducing conditions. Achieving a stable reading for the second sample typically only required a few minutes using this approach.

A test apparatus was designed and constructed to simultaneously maintain numerous actual radioactive samples under either oxidizing or reducing conditions with continuous agitation and gas purge and at constant temperature. A photograph of the test apparatus prior to transfer into the shielded cells is provided in Figure 2-1. Agitation was accomplished using magnetic stir bars and multi-position stir plates obtained from Cole-Parmer. Glass test vessels were constructed in the SRNL glass shop for

controlled-atmosphere testing that would accommodate weekly sub-sampling (see detailed discussion below).

A customized water bath was constructed from 1/2" thick Lexan sheets to fit over two adjacent stir plates and maintain all samples at the target temperature. The glass test vessels were immersed in the water by placing the vessels through fitted slots in the top of the bath which were directly above the sample positions on the stir plates. A rubber gasket was positioned between two Lexan plates on the top of the water bath which resulted in a close fit for the glass test vessels and helped to insulate the bath from the cell environment. The water bath was attached to a temperature-controlled water recirculator (ThermoCube Solid State Cooling System). The recirculator set temperature was maintained at 22 °C throughout testing. Individual sample temperatures were measured using a K-type thermocouple near the end of testing and all samples were found to be 21 °C. A recirculator set temperature of 25 °C (which is the value utilized for waste release modeling) was observed during preliminary equipment evaluations to result in condensation of liquid in the top of the glass vessels during cooler nights in the shielded cells environment. A customized water bubbler manifold was constructed and attached to the back of the water bath in order to monitor and control gas flow through each individual vessel during testing. Low gas supply pressures (typically <5 PSI) were utilized during testing to purge the test vessels. Gas flow control through the vessels was accomplished on the downstream side of each sample gas line by the adjustment of stainless steel Swagelok needle valves. Because the gas outlet lines for each sample were open to the bubbler, the gas pressures in the samples were slightly above atmospheric pressure during leach testing.

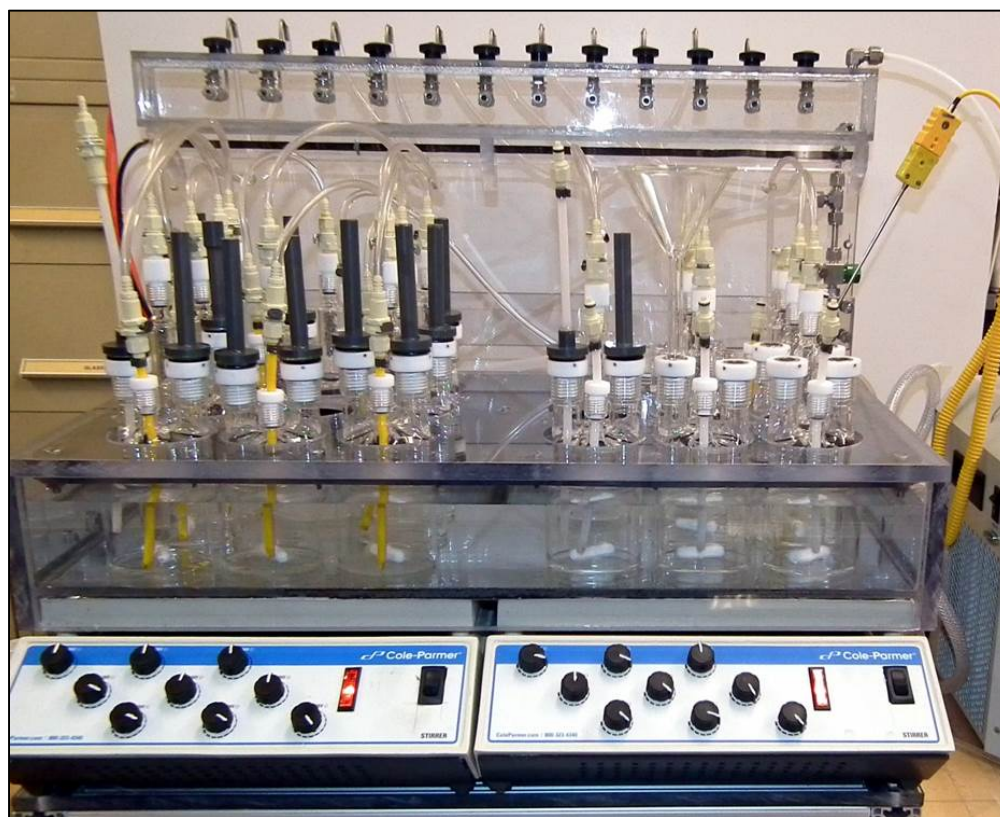


Figure 2-1. Photograph of Testing Equipment Prior to Installation into the SRNL Shielded Cells.

Customized glass test vessels of various types were prepared for testing (see example leach test vessel in Figure 2-2). All test vessels were made of 70.2 mm ID tubing and the main portion of the vessels (excluding the tops) were ~8 cm tall. The vessels would contain ≤ 300 mL of solution. The vessels fit snugly into the sample slots in the top of the customized water bath. Four types of vessels were prepared for testing including: caustic scrubber, humidifier, leach sample, and probe storage vessels. Upper vessel attachments were made from #7 and #15 internal glass screw threads. Threaded Teflon fittings for the screw threads were modified to accommodate the various needed connections. Each vessel top included three to four screw thread fittings. The purpose of the caustic scrubber vessels was to remove carbon dioxide gas from the air supply lines through gas contact with 5 M NaOH solution. Carbon dioxide removal was typically required to avoid impacting the test slurry pH during sample air purging. Each scrubber vessel included a single gas supply line consisting of a 12 mm OD fritted glass gas dispersion tube to promote the formation of numerous gas bubbles and promote gas/liquid contact. A second port with a magnetized cap was included in the scrubber vessel top for the addition of sodium hydroxide reagent. The third and final scrubber vessel attachment included a stainless steel demister suspended within a short glass column for the removal of entrained solution from the outlet gas.

When utilized, the caustic scrubbers were the first vessels that the air was passed through and the gas was then transferred to a humidifier vessel. The purpose of the humidifier vessels was to saturate the supply gas with water vapor at the sample temperature and minimize leach sample evaporation during testing. For oxidizing conditions, the humidifier vessels also served to isolate the leach test samples from the caustic scrubber solution. A single humidifier vessel was utilized to treat the supply gas for each sample type (RRII, ORII, and ORIII) with the water-saturated gas stream then being split between two leach test vessels. Each humidifier vessel included a single gas supply line consisting of 1/4" diameter thin wall polyethylene tubing which had been heat-sealed at the end. Multiple 1/64" holes were drilled into the

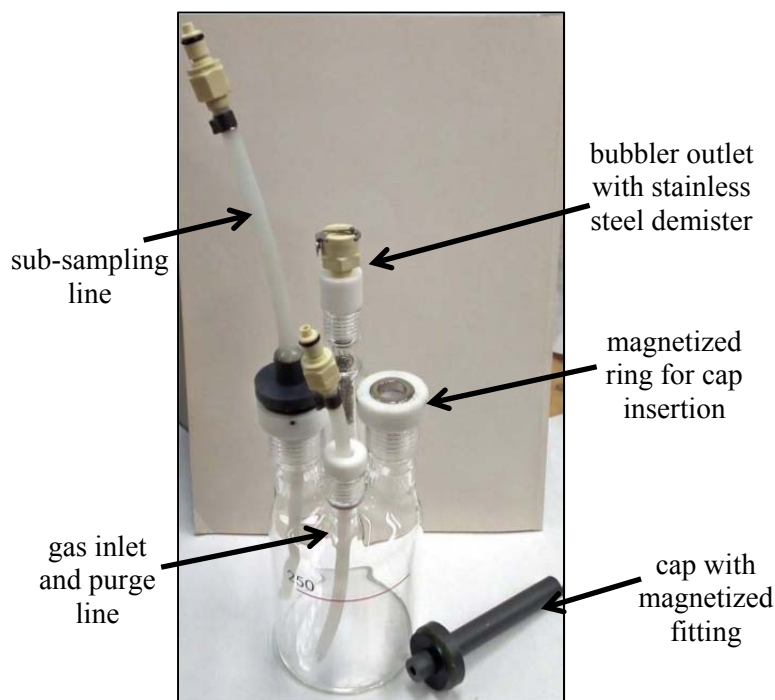


Figure 2-2. Photograph of Leach Testing Sample Vessel.

sides of the tubing near the bottom to produce bubbles and promote gas-liquid contact. The humidifier vessels also included a water addition port with a magnetized cap and two gas outlet lines containing demisters. The outlet lines led to the leach test vessels. The glass leach sample vessels (example shown in Figure 2-2) included a gas supply port, a sample/reagent addition port (magnetized cap), a single gas outlet connection identical in design to the humidifier vessels, as well as a sub-sampling line prepared from 1/4" OD polyethylene tubing. The sample addition port was also used to insert the pH and ORP probes. The tubing on the sub-sampling line extended to within ~1/2" of the vessel bottom and contained a quick-connect fitting at the top to allow for attachment of the sub-sampling system. The probe storage vessel was designed similarly to the other vessels, but included open glass screw threads with no plastic fittings. ORP probes were immersed in water in this vessel when not in use. Reagents and samples were added to the vessels using customized plastic funnels with an attached quick-connect fitting or glass funnels.

A diagram of the vessel layout utilized in the test apparatus is provided in Figure 2-3. Six leach tests were conducted (identified as samples A-F), two vessels for each sample type (RRII, ORII, and ORIII). As indicated in the figure, the gases were passed through a series of vessels for treatment to produce the desired conditions. The vessels in a given series were connected using 1/8" ID Tygon tubing with quick-connect fittings (Colder Product Company PMC12 polypropylene fittings with 1/8" nominal flow) on each end to allow for vessel detachment, removal, or reconfiguration during testing. The sample vessel gas outlet lines were connected to the bubbler system using the same tubing. Control vessels for each sample type (RRII, ORII, and ORIII) were also incorporated into the system in the locations shown. CO₂-stripped air was used as the baseline purge gas for the oxidizing samples (ORII and ORIII). During periods when carbon dioxide was needed to lower the pH, the caustic scrubber was removed from the sequence of vessels that the air was passed through until the target pH was reached. Ultra-high purity nitrogen gas (supplied by cylinder through front wall penetrations) was used as the purge gas for the reducing samples (RRII) throughout testing.

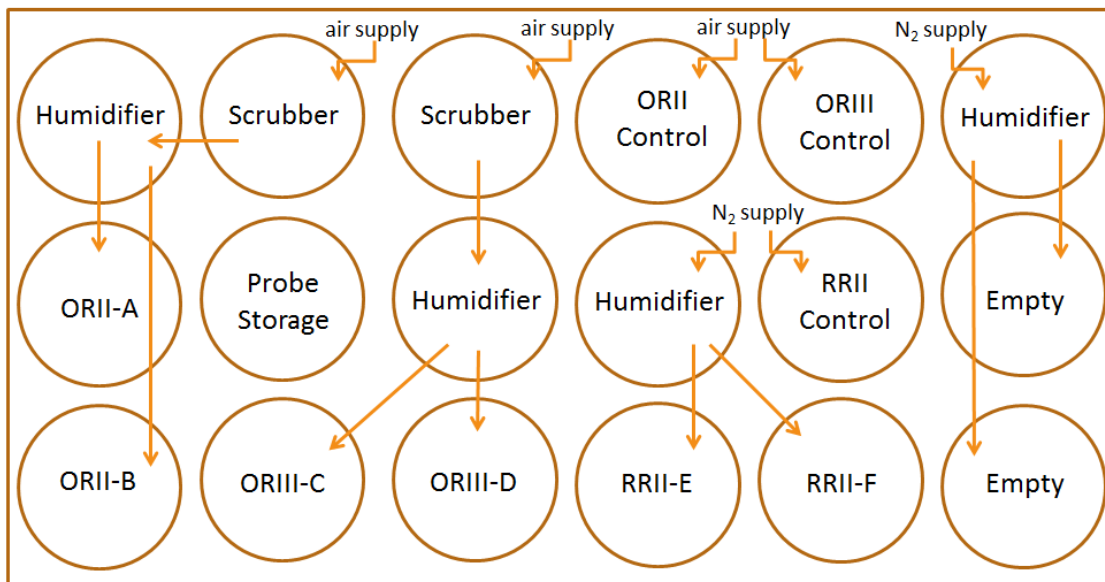


Figure 2-3. Vessel and Plumbing Layout for SRNL Shielded Cells Testing.

Based on the simulant studies and the expected solubilities of most of the metals, it was anticipated that very low solubilities near analysis detection limits would be observed. The need to measure very low concentrations was especially problematic for plutonium, since plutonium contamination of samples in the cells is known due to high background plutonium levels present in the facility. As a result, a sub-sampling system and methodology were developed to allow for the isolation of filtered samples in the analysis bottles. The initial sub-sampling system used is shown in Figure 2-4. The system involved modified, shielded analysis bottles with caps containing ¼" OD polyethylene tubing and quick-connect attachments (same fittings as above). A syringe-based (10-mL, Becton-Dickerson Luer-Lok tip syringe) system was developed using check valves, tee-tube fittings (clear polycarbonate valves and fittings from Nordson Medical Value Plastics; 200 Series barbs with 1/8" fittings), and 1/8" ID Tygon tubing. The equipment functioned like a piston pump, where sample removal from the test vessel was accomplished by pulling back on the syringe plunger after sample system attachment to the vessel sub-sampling line via the quick-connect fitting. This operation pulled liquid through the first check valve. Subsequent pushing on the syringe piston resulted in sample flow diversion through the tee fitting and the second check valve, and then through a 0.1 µm syringe filter (Millex-W PVDF sterile 33 mm with Durapore membrane) directly into the capped analysis bottle (previously attached via quick-connect fitting). The analysis bottle required venting during sample collection via another quick-connect fitting with attached tubing and a second filter, to isolate the sample from contamination on the downstream side. After sample collection, the vent line and the sub-sampling lines were removed from the analysis bottles by depressing the release tabs on the quick-connect fittings. The samples were transferred into fitted foam holders to maintain a vertical orientation during transport to analytical sample receiving. In analytical, care was taken not to contaminate the samples from personnel contact with the bottle exterior surfaces. The sample bottle caps were carefully removed with gloves following general radiological procedures. Then the analyst gloves were changed and sample was removed from the bottle with a pipet without touching the exterior bottle surface. Using this method, the analytical bottles were never opened inside the shielded cells environment and contamination from the bottle surfaces in AD was minimized or eliminated.

As testing continued, the sampling system was simplified due to concerns regarding the volume of sample lost in the transfer lines and inconsistencies in the sample volumes collected. The modified system included a simple syringe with a directly-attached filter (see Figure 2-5). Tubing (1/8") was attached to the downstream side of the filter with a male quick-connect fitting attached to the other end of the tubing. The filter end of the sub-sampling unit was covered with a small plastic bag to minimize the possibility of post-filtration contamination in the cell. The bag was removed just prior to sampling and the syringe filter unit was attached directly to the analytical bottle via the quick-connect fitting. Using this system, the analysis sub-samples were removed from the leach test vessels using a plastic slurry and transferred into the top of the syringe barrel after removing the plunger. Prior to all sampling events, disposable cloth wipes were laid down on the cell floor to minimize contamination. Prior to testing, and periodically during testing, the cell floors were wiped clean to remove contamination.



Figure 2-4. Photograph of Initial Sub-Sampling System and Analysis Sample Vessels with Attached Vent Lines.



Figure 2-5. Photograph of Modified Sub-Sampling System.

2.5 Leaching Studies

A test apparatus was developed and installed in the SRNL shielded cells facility to determine the leaching characteristics of actual radioactive SRS Tank 18F residual solids under conditions believed to be representative of a closed tank during three different periods after tank closure. The leach test slurries included grout-representative solids (CFS or calcium carbonate), Tank 18F residual solids, and ferrous sulfide solids (for reducing samples only). Two liquid simulants were used for testing based on the SIW composition provided in Table 2-2 with calcium carbonate reagent added to each simulant to just beyond

saturation (dusting of solids observed in each simulant). $\text{Ca}(\text{OH})_2$ was added to one simulant sample to produce a solution pH of 11.1 and the resulting simulant was utilized for ORII and RRII testing. Air sparging of a second simulant sample resulted in a solution pH near 9.2 and this simulant was utilized for ORIII testing. Residual soluble salts in the actual Tank 18F solids resulted in elevated pH and elevated sodium levels relative to the initial SIW composition. As a result, except for selected tests it was necessary to wash the solids with simulant to remove the residual soluble salts. Sample washing was conducted for samples A through D (test conditions ORII and ORIII) prior to leach testing. Wash solutions were in contact with the test samples for several days prior to removal from the vessels. Sample washing was not conducted for samples E and F (RRII conditions) until after the completion of three weeks of leach testing. This two-phased approach was expected to be representative of the earlier and latter portions of the RRII phase of aging. During leach studies the test samples were continuously agitated with magnetic stir bars and purged with either nitrogen, air, or CO_2 -stripped air. Testing was conducted at 21-22 °C over a period of approximately two months with sub-samples being collected approximately weekly.

The dissolution of Pu, U, Tc, and Np present in Tank 18F residual solids mixed with calcium carbonate or CFS solids and, for reducing cases, ferrous sulfide solids were evaluated in the grout pore water simulant solutions prepared as described in Section 2.2. CFS and calcium carbonate solids were added to each test sample at a concentration of 16.7 ± 0.1 g/L. Tank 18F solids were added to each test sample at a concentration of 30.1 ± 0.2 g/L. This phase ratio was selected based on a combination of solubility and analytical limit of detection considerations and not the actual condition in a grout-filled tank. A goal in selecting the phase ratio was ensuring that key dose contributors were not removed to any appreciable extent by the pore water flow prior to reaching the ORIII condition. FeS solid was added to RRII samples at a concentration of 3.1-3.2 g/L. Slurry volumes ranged from 200-250 mL. Test samples were prepared by the addition of various solid reagents and simulant solutions (see Table 2-6) to the test vessels after equipment installation in the shielded cells. The A and B leach samples were replicate samples for the ORII condition. The C and D samples were also initially replicate samples for the ORIII condition, until the D sample was compromised during testing (see discussion below). The E and F samples were both intended to represent the RRII condition, but with different grout-representative phases (calcium carbonate for Sample E; CFS solids for Sample F). In addition to the reagents listed in Table 2-6, calcium hydroxide was added as needed to raise the pH of the ORII and RRII samples to near the target values. An air purge (without CO_2 removed) was utilized to lower the pH of the oxidizing samples (ORIII in particular), as needed.

The dates of sample preparations and sub-sampling and comments regarding the testing are provided in Table 2-7. Initial sample preparations and conditioning were conducted 2-3 weeks prior to the test start date. Soon after contacting the RRII samples with pore water simulant solutions, the vessels were placed under nitrogen to avoid exposing the samples to ambient oxidizing conditions. Since the ORII and ORIII sample types represent the grout aging stages where many volumes of pore water have passed through the system, samples A-D were washed with two portions of the appropriate simulant solutions prior to the initiation of leaching studies. The decant wash volumes isolated from each sample are provided in Table 2-8. Scoping studies indicated that the wash volumes used would decrease the soluble sodium concentration to near that of the as-prepared simulant composition. The RRII samples (E and F) were not washed initially, since this condition represents the early portion of grout aging. After approximately three weeks of leach testing and sub-sampling, the liquid was decanted from each of the RRII samples and fresh simulant was added. As a result, RRII testing was conducted in two phases with the second testing phase involving lower solution ionic strength. Leach test samples were monitored during testing to evaluate whether evaporative or entrainment sample losses associated with continuous sample gas purging were an issue. After three weeks of testing, the liquid heights of selected samples were measured and it was confirmed that sample losses were minimal. During the entire course of the leaching studies, 30-50 volume percent of the initial sample slurries was consumed due to sub-sampling.

2.6 Sample Analysis

Sample aliquot volumes of 5-13 mL (depending on the volume needed for analysis) were collected from the leaching test vessels for analysis after the measurement of the solution pH and E_h at approximately weekly intervals. Seven sampling events were conducted over a period of nearly two months (sub-sample collection days: 9, 16, 23, 27, 37, 44, and 51). The aliquots were filtered as described above through 0.1- μ m poly vinyl difluoride (PVDF) syringe filter units without opening the bottle caps. Blank sample analysis generally indicated that contamination from the cell environment was minimal for all metals analyzed, although uranium was consistently observed in sample blanks at relatively low levels. 5 M nitric acid volumes of 0.5-1.5 mL (adjusted for the target sample volume to give an acid:sample volume phase ratio near 8) were placed in the analysis bottles prior to cell entry to acidify the samples and avoid post-filtration precipitation. Aliquots of the acidified samples were analyzed for plutonium by alpha spectroscopy following separation using thenoyltrifluoroacetone (TTA) and for uranium, technetium, and neptunium by Inductively Coupled Plasma Mass Spectrometry (ICP-MS). Reported plutonium concentrations are based on the measured combined Pu-239/Pu-240 concentrations in dpm/mL converted to molar concentrations assuming 100% Pu-239. Pu-238 concentrations were negligibly small (on a molar concentration basis) for all samples.

Other analyses were conducted on selected samples including: Inductively Coupled Plasma Emission Spectroscopy (ICP-ES), Ion Chromatography (IC; for oxalate anion), gamma scan (for Cs-137), beta scintillation counting (for Sr-90 and Tc-99), and alpha/gamma pulse height analysis (APHA/GPHA; for Am). Selected wash solutions were filtered and analyzed by ICP-MS and IC anion. Sub-samples of selected solid test samples were collected at test conclusion and analyzed with a sample of the original solids by X-ray Diffraction (XRD), Scanning Electron Microscopy (SEM), and Particle Size Determination (PSD). Separate solid sub-samples were digested in acid (sodium peroxide fusion) to determine the elemental composition by ICP-MS and ICP-ES.

All sample chemical and physical analyses (excluding pH and ORP) were conducted by the SRNL Analytical Development (AD) section.

2.7 Quality Assurance

Requirements for performing reviews of technical reports and the extent of review are established in Manual E7 2.60. SRNL documents the extent and type of review using the SRNL Technical Report Design Checklist contained in WSRC-IM-2002-00011, Rev. 2. All pertinent instructions results and calculations were recorded in an Electronic Laboratory Notebook (ELN) experiment in accordance with the ELN Implementing Plan.⁹ Instructions and data are recorded in SRNL Electronic Notebook: A2341-00117-04, SRNL Electronic Notebook (Production); SRNL, Aiken, SC 29808 (2014).

Table 2-6. Test Sample and Reagent Masses and Solution Volumes.

Sample ID	Tank 18F Residual (g)	CaCO₃ (g)	FeS (g)	CFS (g)	Simulant Type	Simulant Volume (mL)
ORII-A	6.016	3.332	---	---	ORII/RRII	200
ORII-B	6.068	3.346	---	---	ORII/RRII	200
ORIII-C	6.013	3.352	---	---	ORIII	200
ORIII-D	6.034	3.341	---	---	ORIII	200
RRII-E	7.482	4.191	0.763	---	ORII/RRII	250
RRII-F	7.559	---	0.794	4.175	ORII/RRII	250

Table 2-7. Test Sample Preparation and Sub-Sampling Timeline and Comments.

Date	Activity	Comments
3/15	sample preparation	sample preparation initiated
3/23	sample preparation	all samples in vessels
3/29	sample conditioning	transferred first portion of FeS reagent to E and F samples
3/29	sample conditioning	first wash of A-D samples (150 mL per sample)
3/30	sample conditioning	second wash of A-D samples (150-165 mL per sample)
4/5	test start	
4/13	sample conditioning	transferred second portion of FeS reagent to E and F samples
4/14	1 st sub-sampling	inadvertently transferred bubbler water into D sample
4/21	2 nd sub-sampling	no D sub-sample; reconditioning D sample with fresh simulant
4/28	3 rd sub-sampling	resumed sampling of D sample, simplified sub-sampling method used
5/2	sample conditioning	decant simulants from E and F samples and add 250 mL fresh simulant
5/5	4 th sub-sampling	---
5/12	5 th sub-sampling	---
5/19	6 th sub-sampling	---
5/26	7 th sub-sampling	---

Table 2-8. Test Sample Wash Decant Volumes.

Date	Volume (mL)	Comments
ORII-A	600	wash conducted prior to leach testing
ORII-B	650	wash conducted prior to leach testing
ORIII-C	600	wash conducted prior to leach testing
ORIII-D	1600	600 mL wash conducted prior to leach testing, additional wash following sample compromise from bubbler water
RRII-E	595	wash conducted following leach test week three
RRII-F	500	wash conducted following leach test week three

3.0 Results and Discussion

A photograph of the sludge leaching test apparatus after installation into the shielded cells and after addition of the leach test samples is provided in Figure 3-1. Slurry pH and E_h data and metal concentrations for filtered sub-samples obtained throughout the seven week testing period are provided in Table 3-1. Missing data in the table for some samples during the first three weeks was the result of sample or sub-sampling issues during testing. A photograph showing the various test vessels (scrubber, humidifier, and leach sample vessels) at the conclusion of leach testing is provided in Figure 3-2. Analysis results for control samples are provided in Table 3-2. The slurry pH and E_h data collected throughout the testing are plotted versus the experiment time (in days) in Figures 3-3 and 3-4, respectively. The target pH values were achieved to within 0.5 pH units for all samples. Leaching studies were conducted over an E_h range of approximately 0.7 V. However, the highest and lowest E_h values achieved of $\sim+0.5$ V and ~-0.2 V were significantly less positive and less negative, respectively,

than the target values. These experimental limitations are attributed to the presence of multiple solid phases and the relatively slow reaction kinetics for the conversion of solid phases under the tests conditions. As previously reported with simulated tank waste solids, more positive and more negative E_h values required the addition of non-representative oxidants and reductants, respectively. As was the case during simulant testing, the highest E_h values were observed for the ORIII test samples and the lowest values were observed for the RRII samples. Higher E_h values were observed for the early RRII samples prior to sample washing which was conducted between the third and fourth testing weeks. Presumably, the higher E_h values are associated with the higher ionic strength of the samples prior to washing.

Plutonium concentrations of the oxidizing ORII and ORIII leach test sub-samples as a function of collection time in days are provided in Figure 3-5. A gradual increase in Pu concentration was observed for both ORII test samples versus time, and it is unclear based on the data whether saturation and equilibrium were achieved during the testing period. In addition, the Pu concentrations observed for the ORII-A sub-samples were consistently an order of magnitude lower than the ORII-B samples. This difference is not understood, since nearly identical sample preparation methods and amounts were used for each sample. Plutonium concentrations observed for the ORIII test samples (C and D) were more stable and were typically the highest values observed (near $1E-8$ M) of any samples tested. Due to the gradual increases observed for the ORII-B samples, the final sub-sample analyzed was also near $1E-8$ M. Plutonium concentrations observed for the reducing RRII case are provided in Figure 3-6, where the earlier unwashed test samples are indicated by -1 and the latter washed samples are indicated by -2. The RRII-F samples were consistently lower than the RRII-E samples by about an order of magnitude, presumably due the presence of the CFS solids in the RRII-F sample. Lower plutonium concentrations were also observed for simulant samples containing CFS solids in previous testing.⁶ Early F samples exhibited a rapid increase in plutonium concentration each week. After sample washing, the Pu concentrations for the F samples (prior to washing) stabilized near $1E-10$ M. The Pu concentrations for the E samples ranged from $1E-9$ to $5E-9$ M throughout the testing period. Only one control sample (44 days) contained plutonium above detectable limits (Table 3-2), and this sample contained plutonium at levels just above detection and well below most leach test sample results. This observation indicates that the test methodology and sub-sample design successfully eliminated plutonium contamination and the plutonium concentrations observed for the samples can be attributed to the metal leaching from the Tank 18F residual solids.

Table 3-1. Measured pH and E_h Data and Metal Concentrations for Each Pore Water Condition with Actual Tank 18F Residual Solids.

Sample	Week	pH	E _h (mV)	Pu (M)	U (M)	Tc (M)	Np (M)
ORII-A	1	11.4	330	6.0 E-11	1.8E-06	<5.4 E-09	<2.3 E-09
	2	11.3	391	<1.2 E-10	2.6 E-06	3.3 E-09	<2.4 E-10
	3	11.4	356	9.3 E-11	---	---	---
	4	11.4	402	1.7 E-10	3.2 E-06	7.7 E-09	<2.4 E-09
	5	11.2	324	4.0 E-10	4.3 E-06	9.5 E-09	<2.4 E-10
	6	11.2	320	4.7 E-10	4.3 E-06	1.1 E-08	<2.4 E-10
	7	11.1	358	5.7 E-10	3.6 E-06	1.3 E-08	<2.4 E-10
ORII-B	1	11.0	311	8.2 E-10	2.9 E-06	<5.5 E-09	<2.3 E-09
	2	11.0	291	2.6 E-09	3.8 E-06	6.6 E-09	<2.4 E-10
	3	10.9	407	3.0 E-09	3.5 E-06	8.1 E-09	<1.2 E-09
	4	10.9	342	4.2 E-09	4.0 E-06	8.8 E-09	<2.4 E-09
	5	11.0	309	5.0 E-09	6.8 E-06	9.2 E-09	<2.4 E-10
	6	10.8	317	5.0 E-09	1.6 E-05	1.1 E-08	2.7 E-10
	7	10.6	343	8.5 E-09	4.2 E-05	1.3 E-08	3.4 E-10
ORIII-C	1	9.6	354	1.0 E-08	2.3 E-04	<5.5 E-09	4.5 E-09
	2	9.6	304	1.6 E-08	2.7 E-04	4.8 E-09	4.2 E-09
	3	9.5	520	1.7 E-08	2.6 E-04	7.8 E-09	4.6 E-09
	4	9.2	522	1.1 E-08	3.7 E-04	8.0 E-09	4.2 E-09
	5	9.2	474	1.2 E-08	4.2 E-04	8.5 E-09	4.8 E-09
	6	9.5	536	9.8 E-09	3.9 E-04	1.1 E-08	3.2 E-09
	7	9.7	549	7.9 E-09	3.3 E-04	1.2 E-08	3.0 E-09
ORIII-D	1	9.8	348	2.0 E-08	1.6E-04	<5.5 E-09	7.9 E-09
	2	---	---	---	---	---	---
	3	9.0	520	3.2 E-09	5.0 E-06	<2.9 E-09	<1.4 E-09
	4	9.0	472	7.6 E-09	9.5 E-05	<5.7 E-09	<2.4 E-09
	5	9.1	511	8.6 E-09	6.5 E-05	4.4 E-09	1.5 E-09
	6	9.5	516	4.8 E-09	6.2 E-05	6.3 E-09	1.2 E-09
	7	9.5	472	4.5 E-09	4.7 E-05	6.3 E-09	1.3 E-09
RRII-E	1	11.0	59	---	---	---	---
	2	10.9	-159	7.8 E-10	6.5 E-04	1.7 E-09	8.5 E-10
	3	10.9	-43	7.4 E-10	5.9 E-04	<2.9 E-09	<1.2 E-09
	4	10.9	-174	7.7 E-10	1.1 E-06	<5.7 E-09	<2.4 E-09
	5	10.9	-244	4.5 E-09	1.7 E-06	<5.7 E-10	<2.4 E-10
	6	10.9	-262	2.8 E-09	2.8 E-06	<5.6 E-10	<2.4 E-10
	7	10.9	-153	1.8 E-09	2.7 E-06	<5.7 E-10	<2.4 E-10
RRII-F (CFS)	1	11.7	-29	2.5 E-12	1.3 E-05	1.1 E-08	<2.3 E-09
	2	11.7	-321	<1.4 E-11	1.1 E-05	3.0 E-09	<2.4 E-10
	3	11.7	-174	1.4 E-10	1.1 E-05	<2.9 E-09	<1.2 E-09
	4	11.3	-199	1.1 E-10	2.2 E-06	<5.8 E-09	<2.4 E-09
	5	11.4	-249	4.5 E-11	1.9 E-06	<5.7 E-10	<2.4 E-10
	6	11.4	-202	9.1 E-11	1.6 E-06	<5.6 E-10	<2.3 E-10
	7	11.4	-135	3.3 E-11	1.5 E-06	<5.7 E-10	<2.4 E-10

Table 3-2. Leaching Study Control Sample Analysis Results.

Days	Control Sample	Pu (M)	U (M)	Tc-99 (M)	Np-237 (M)
9	C	<1.1 E-11	<2.3 E-09	<5.5 E-09	<2.3 E-09
16	A	<1.3 E-10	<1.7 E-09	<5.7 E-10	<2.4 E-10
23	C	<2.7 E-11	4.6 E-08	<3.0 E-09	<1.2 E-09
27	C	<1.4 E-10	1.3 E-07	<5.7 E-09	<2.4 E-09
44	A	1.2 E-11	4.1 E-10	<5.6 E-10	<2.4 E-10
51	A	<9.9 E-12	7.2 E-10	<5.7 E-10	<2.4 E-10

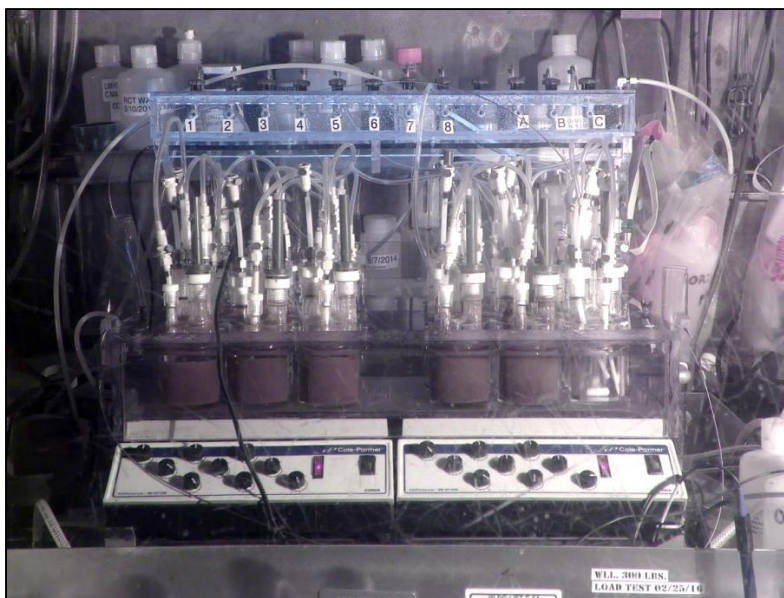


Figure 3-1. Photograph of Testing Equipment After Installation in the SRNL Shielded Cells and After Sample Addition/Preparation.

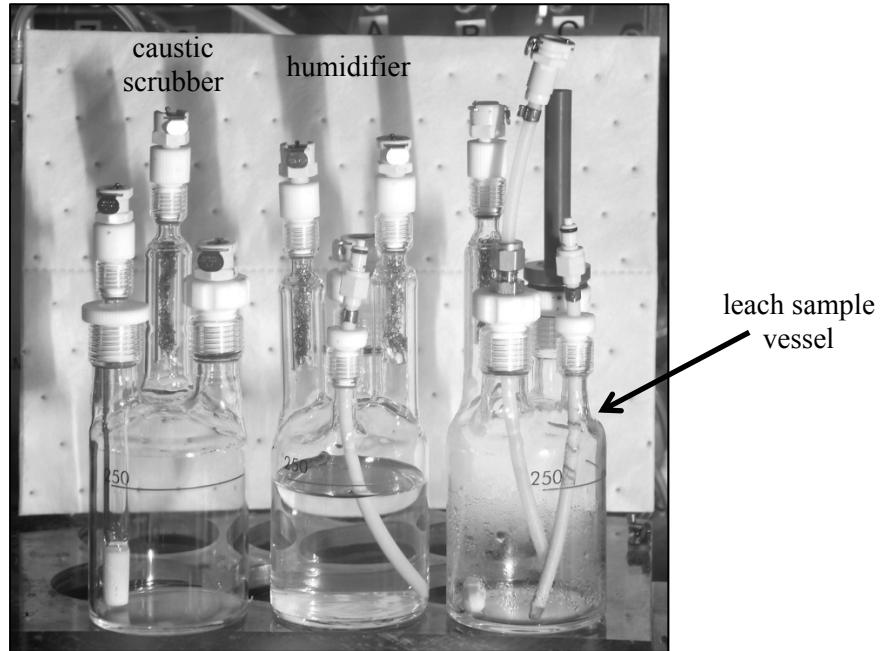


Figure 3-2. Photograph of Test Vessels in the SRNL Shielded Cells at Test Conclusion (sample/reagents removed).

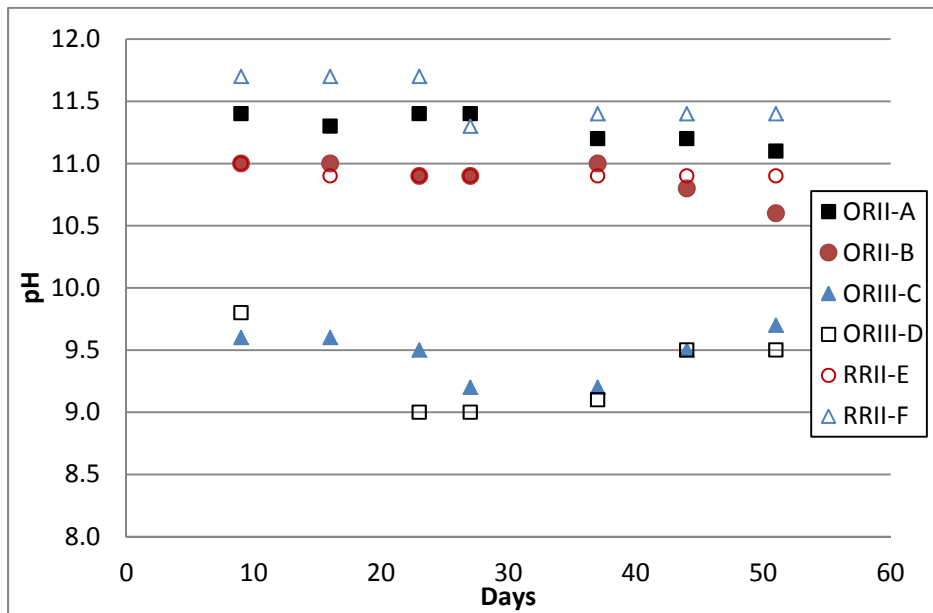


Figure 3-3. Slurry pH Data Collected During Tank 18F Residual Solids Leaching Studies.

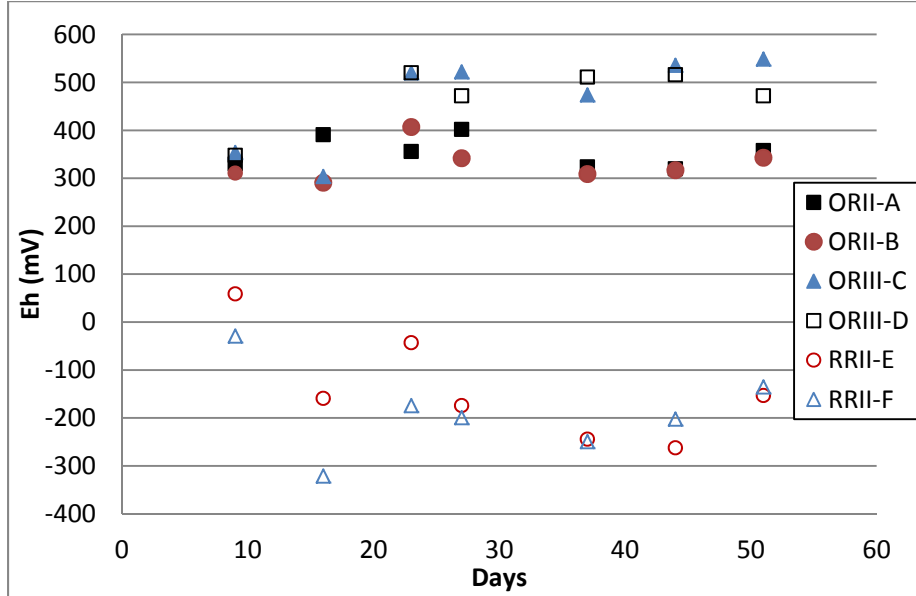


Figure 3-4. Slurry Eh Data Collected During Tank 18F Residual Solids Leaching Studies.

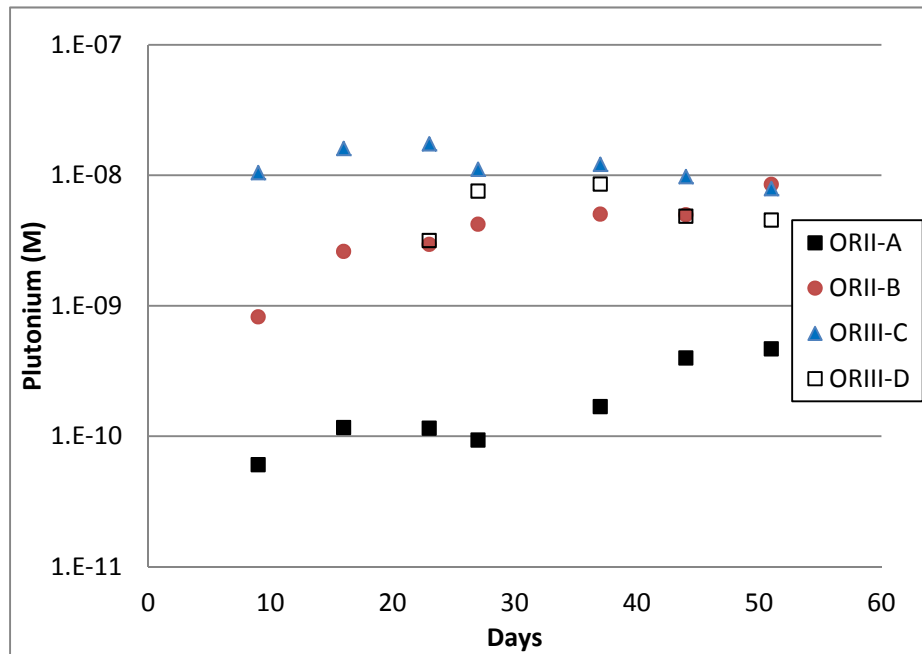


Figure 3-5. Plutonium Concentrations Versus Time During Tank 18F Residual Solids Leaching Studies for Oxidizing Conditions (ORII and ORIII).

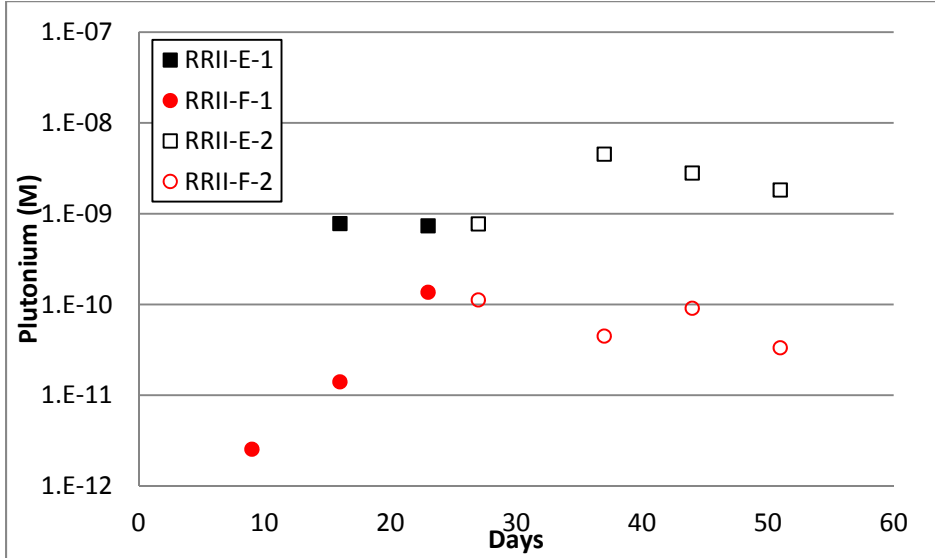


Figure 3-6. Plutonium Concentrations Versus Time During Tank 18F Residual Solids Leaching Studies for Reducing Conditions (RRII). Note: Data labeled as -1 and -2 was collected prior to and after the final wash, respectively.

Table 3-3. Estimated Maximum Metal Losses to Tank 18F Residual Washes Prior to Leach Testing.

Maximum Total Losses to Wash (%)				
Sample	Pu	U	Np	Tc
ORII-A	0.18	16	0.57	6.5
ORII-B	0.18	16	0.57	6.4
ORIII-C	0.17	15	0.55	6.2
ORIII-D	0.46	40	1.5	17
RRII-E	0.14	12	0.44	5.0
RRII-F	0.11	10	0.36	4.1

* calculated losses based on wash volumes and assuming maximum observed concentrations during leach testing

The unusually low Pu concentrations observed for sample ORIII-D (Figure 3-5; D sub-samples averaged 62% of ORIII-C sub-samples over final 4 testing weeks) were not expected given the fact that this test condition would be expected to exhibit the highest actinide concentrations. The concentration observed for the final D sample is actually lower than the final value observed for the RRII-E reducing sample. The lower concentration for the D sample is believed to have been associated with the excessive washing of the sample following the inadvertent flooding of this sample from the bubbler system during the first sampling event. Conservatively estimated (maximum) losses of the various metals of interest to the wash solutions based on the wash volumes and assuming the maximum observed metal concentrations during leach testing are provided in Table 3-3. As shown in the table, the estimated plutonium loss to the wash solutions was greatest for the D sample due to the larger wash volume for this sample (Table 2-8). However, the estimated fraction of Pu removed was still small (<0.5%), as would be expected. Based on this observation, it would appear that the residual sample may include two types of plutonium with differing solubilities. The different solubilities could be associated with oxidation state, chemical speciation, or matrix differences. For example, a significant fraction of the plutonium in the sample could be co-precipitated with other metals present in the residual solids or imbedded deep within the solid matrix.

Measured uranium concentrations for the oxidizing samples (ORII and ORIII) are plotted versus time in Figure 3-7. The uranium concentrations for all test samples were much higher than the concentrations observed for the other metals. The highest uranium concentration was observed for the ORIII-C sample where the uranium ranged from $2\text{E-}4$ to $5\text{E-}4$ M. The ORIII-D sub-samples contained significantly lower uranium concentrations than the C samples in all cases. This is believed to be due to the additional washing of the D sample discussed above. As shown in Table 3-3, as much as 40% of the total uranium present in the Tank 18F residual sample may have dissolved during sample washing. Uranium leaching from sludge samples is often observed during tank washing operations. The ORII-A and ORII-B sub-samples contained significantly lower uranium concentrations than the ORIII-C sample. The A and B sub-samples were quite similar during the first thirty days of sampling and appeared to be stable. After 30 days, the uranium concentrations in the B sub-samples increased significantly while the concentrations for the A samples were more constant. The differences between the A and B samples are not understood. Uranium concentrations observed for the reducing RRII case are provided in Figure 3-8, where the earlier unwashed test samples are indicated by -1 and the later washed samples are indicated by -2. Dramatic differences were observed in the uranium concentrations before and after sample washing, with the concentrations after washing being one to two orders of magnitude lower than the concentrations before washing. The uranium concentrations observed at 16 and 24 days for the RRII-E sample were higher than the concentrations observed for any other samples, including the ORIII samples. Subsequent analysis of selected wash samples provided some insight into the higher elevated uranium concentrations for these samples (see discussion below). Before washing, the concentrations observed for the RRII-F-1 samples were much lower than the RRII-E-1 sub-samples, presumably due to the presence of the CFS solids. After washing (-2 samples), the E and F sub-samples contained similarly low and stable uranium concentrations ranging from $1\text{E-}6$ to $3\text{E-}6$ M. Surprisingly, the control sample analysis indicated that uranium contamination occurred for the later control samples. However, the highest uranium concentration in the control samples of $1\text{E-}7$ M is significantly lower than all leach test sample concentrations observed.

The technetium concentrations observed for the leach test sub-samples from the oxidizing samples (ORII and ORIII) versus time are provided in Figure 3-9. Very similar results were observed for the A, B, and C samples, while lower concentrations were observed for the D sub-samples, presumably due to the fact that 17% of the sample technetium may have been lost from this sample during washing (Table 3-3). The data trends in the technetium concentrations indicate that the technetium concentration did not stabilize during testing but continued to slowly increase. No measurable technetium was observed for any of the

reducing samples (RRII-E and RRII-F concentrations $<6 \text{ E-10 M}$). In addition, no detectable technetium was observed for any control samples.

Neptunium concentrations observed for the leach test sub-samples from the oxidizing samples (ORII and ORIII) versus time are provided in Figure 3-10. The highest neptunium concentrations were typically observed for the C sample (except for the first D sub-sample), while the concentrations for most of the D sub-samples were significantly lower. The maximum estimated loss to the washes for the D sample was only 1.5%. As was the case for plutonium, the results appear to indicate that the samples may include two types of neptunium with differing solubilities. No measurable neptunium was observed for any of the reducing samples (RRII-E and RRII-F) or for sample ORII-A (concentrations $<3\text{E-10 M}$). In addition, no detectable neptunium was observed for any control samples.

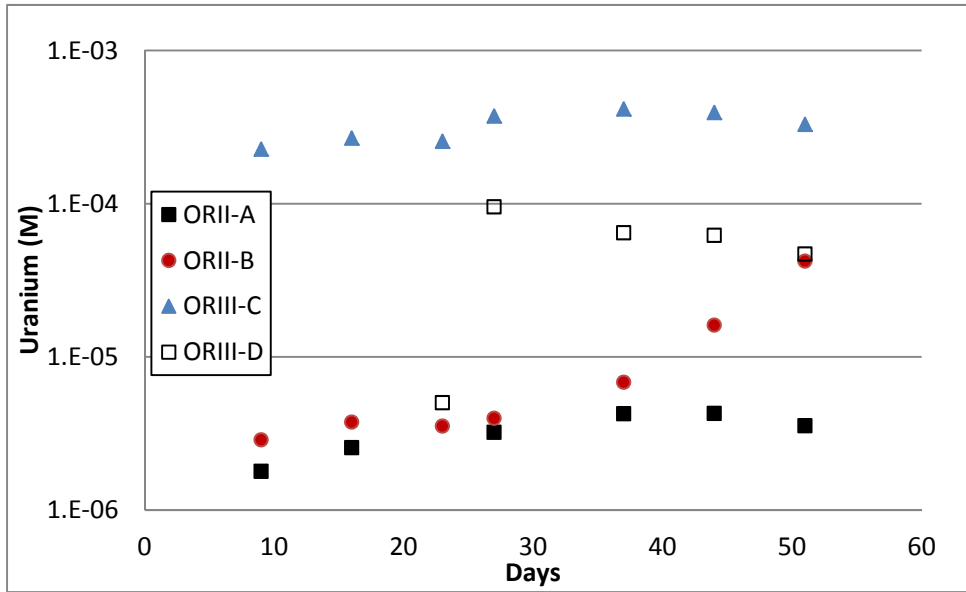


Figure 3-7. Uranium Concentrations Versus Time During Tank 18F Residual Solids Leaching Studies for Oxidizing Conditions (ORII and ORIII).

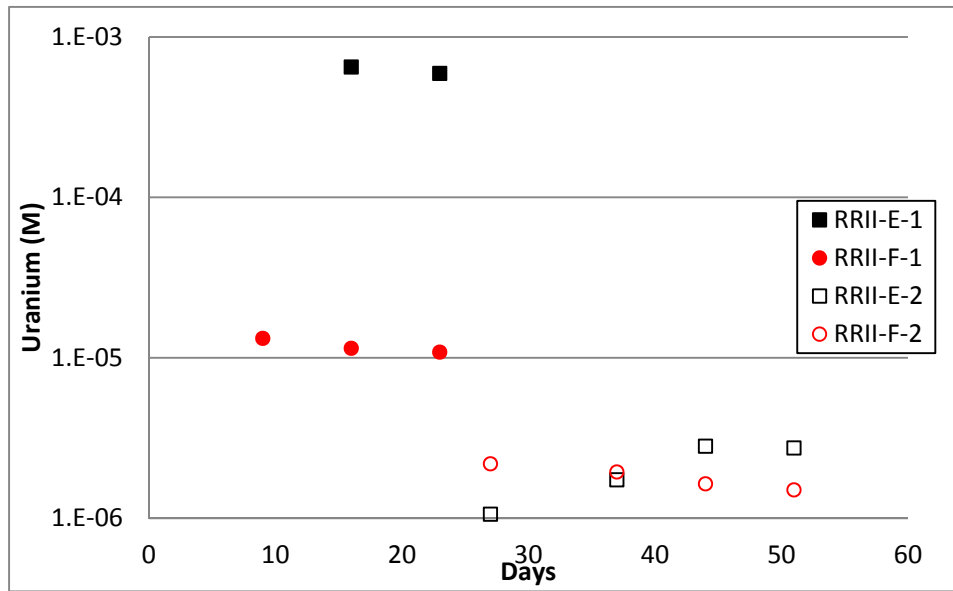


Figure 3-8. Uranium Concentrations Versus Time During Tank 18F Residual Solids Leaching Studies for Reducing Conditions (RRII).

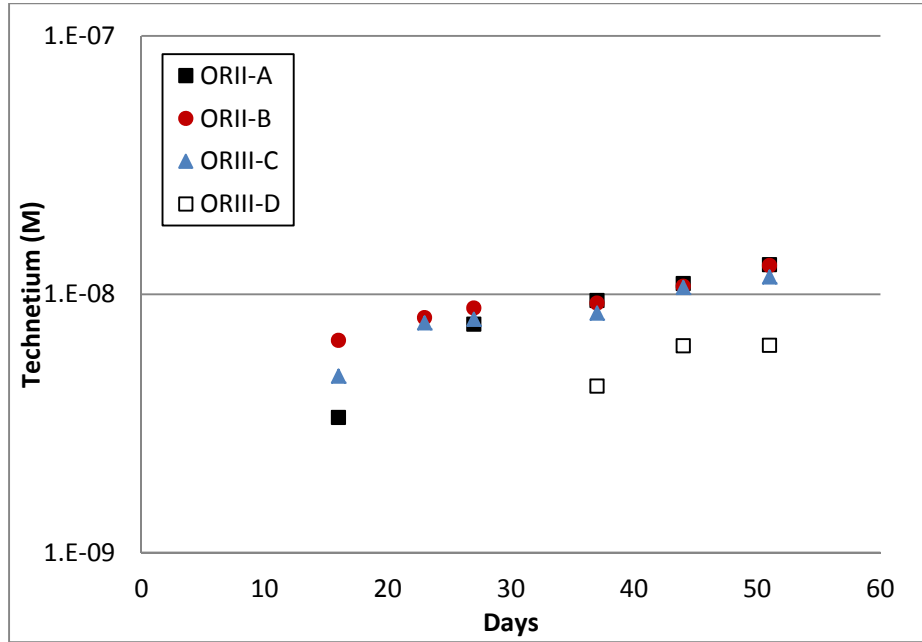


Figure 3-9. Technetium Concentrations Versus Time During Tank 18F Residual Solids Leaching Studies for Oxidizing Conditions (ORII and ORIII).

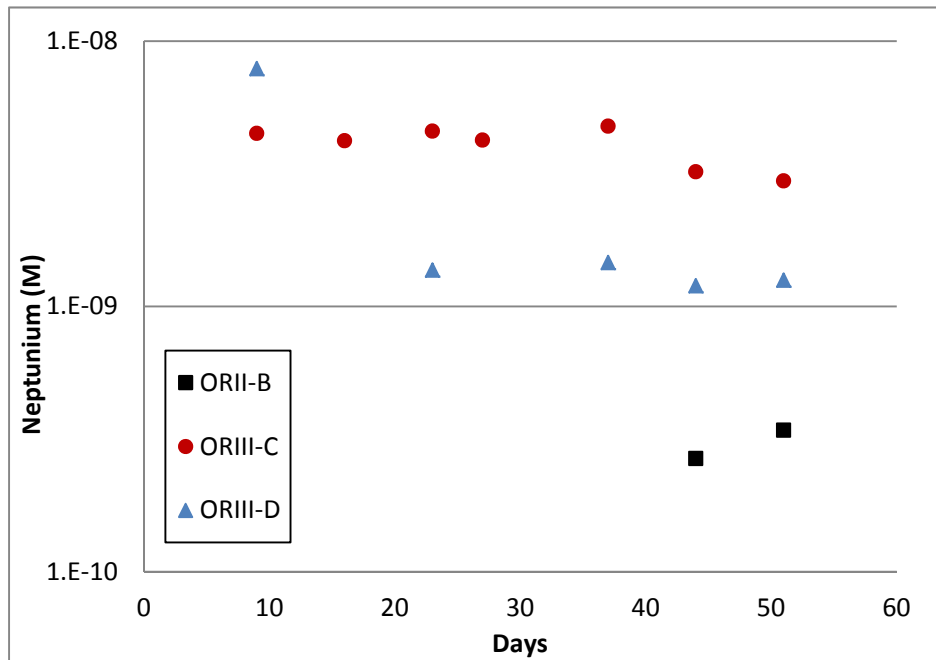


Figure 3-10. Neptunium Concentrations versus Time during Tank 18F Residual Solids Leaching Studies for Oxidizing Conditions (ORII and ORIII).

A summary of predicted solubilities for assumed plutonium and uranium species reported by Denham² at various E_h values is provided in Table 3-4. The E_h values include the target values for each condition provided in Table 2-3. For the oxidizing cases (ORII and ORIII), the target conditions provided in Table 2-3 assume equilibrium with dissolved oxygen. In addition, actinide solubilities were calculated for the oxidizing samples for the more realistic cases where equilibrium with dissolved oxygen does not exist and the E_h values are lower. The more realistic E_h values were +240 mV for the ORII condition and +290 mV for the ORIII condition. The highest experimentally observed E_h value for ORII was +291 mV and the highest value observed for ORIII was +549 mV. These data are intermediate between the values used by Denham for these conditions. Solubility predictions were calculated for pure Pu and U phases and apparent solubilities were calculated for the actinides co-precipitated with Fe phases. The apparent solubilities are based on the primary iron phase solubility and the ratio of the actinides to the iron phase. In all cases, the predicted uranium solubility is greater than the plutonium solubility. Predicted apparent solubilities for the co-precipitated phases are much lower than the solubilities for the pure phases. The highest Pu solubility (8E-08 M) is predicted for the ORIII condition in equilibrium with dissolved oxygen. The highest U solubility (6E-05 M) is predicted for the ORII condition in equilibrium with dissolved oxygen. The initial assumed Pu phase was hydrous, amorphous PuO_2 , however, it is reported that E_h values above +450 mV for ORII and +530 mV for ORIII result in conversion of increasingly greater amounts of the Pu to higher oxidation states, such that the solubility-controlling phase near +600 mV is the Pu(VI) phase, $\text{PuO}_2(\text{OH})_2 \cdot \text{H}_2\text{O}$. The sensitivity of U solubility to E_h is almost a step change with similar predicted changes in uranium speciation. Below an E_h of approximately -400 mV, the controlling phase is U(IV) oxide (UO_2) and solubility is predicted not to vary with more reducing E_h values. Above an E_h of approximately -200 mV, the much more soluble U(VI) phase, $\text{UO}_3 \cdot 2\text{H}_2\text{O}$, dominates and the U solubility is predicted not to vary with increasing (i.e., more oxidizing) E_h values such as those represented by ORII and ORIII.

Average experimentally observed pH, E_h , and leachate metal concentrations for each test sample are provided in Table 3-5. The pH values were within <0.5 pH units of the target values for all samples. The experimentally observed average E_h value for the two RRII samples was -201 ± 8 mV. The experimentally observed average E_h value for the two ORII samples was $+340 \pm 12$ mV. The experimentally observed average E_h value for the two ORIII samples was $+507 \pm 14$ mV. Based on these results, the speciation would be expected to be dominated by the hydrous, amorphous PuO_2 phase and the very soluble U(VI) phase, $\text{UO}_3 \cdot 2\text{H}_2\text{O}$ across the range of test conditions.

Table 3-4. Predicted Solubilities of Assumed Pu and U Phases.

Condition	Initial Phase	E_h (mV)	Pu (M)	U (M)
RRII ^a	PuO_2^d or UO_2	-470	3E-11	5E-09
RRII ^c	Magnetite co-precipitate	-470	8E-13	2E-12
ORII ^a	PuO_2^d or $\text{UO}_3 \cdot 2\text{H}_2\text{O}$	+240	3E-11	5E-05
ORII ^b	PuO_2^d or $\text{UO}_3 \cdot 2\text{H}_2\text{O}$	+560	5E-08	6E-05
ORII ^c	Maghemite co-precipitate	+240	7E-12	2E-11
ORIII ^a	PuO_2^d or $\text{UO}_3 \cdot 2\text{H}_2\text{O}$	+290	3E-11	4E-06
ORIII ^b	PuO_2^d or $\text{UO}_3 \cdot 2\text{H}_2\text{O}$	+680	8E-08	4E-06
ORIII ^c	Maghemite co-precipitate	+290	1E-13	5E-13

^a from Table 11 of SRNL-STI-2012-00404²; E_h values represent more realistic, non-equilibrium conditions with dissolved oxygen

^b from Table 12 of SRNL-STI-2012-00404²; E_h values represent equilibrium conditions with dissolved oxygen

^c from Table 14 of SRNL-STI-2012-00404²; represents apparent solubility based on primary iron phase solubility and Fe:Pu:U ratio

^d solubility based on hydrous, amorphous plutonium oxide phase

Table 3-5. Measured pH, E_h, and Metal Concentrations for Each Pore Water Test Condition Using Actual Tank 18F Residual Solids.

Test Condition	Sample ID	Additives	Atmosphere	E _h ^a (mV)	pH ^a	Pu ^a (M)	U ^a (M)	Tc ^a (M)	Np ^b (M)
RRII	E	Ca(OH) ₂ , CaCO ₃ , FeS	continuous N ₂ purge	-208	10.9	2E-9	2E-6 ^d	<6E-10	<2E-10
RRII	F	CFS ^c , FeS	continuous N ₂ purge	-196	11.4	7E-11	2E-6 ^d	<6E-10	<2E-10
ORII	A	Ca(OH) ₂ , CaCO ₃	continuous air purge	+351	11.2	4E-10	4E-6	1E-8	<2E-10
ORII	B	Ca(OH) ₂ , CaCO ₃	continuous air purge	+328	10.8	6E-9	2E-5	1E-8	3E-10
ORIII	C	CaCO ₃	continuous air or CO ₂ -stripped air purge	+520	9.4	1E-8	4E-4	1E-8	4E-9
ORIII	D	CaCO ₃	continuous air or CO ₂ -stripped air purge	+493	9.3	6E-9	7E-5	6E-9	1E-9

^a average data from final 4 weeks

^b average data from final 2-3 weeks

^c CFS = cement, fly ash, and slag grout solids

^d much higher U concentrations were observed for unwashed samples (1E-5 to 6E-5 M)

Comparison of the average results observed experimentally for Pu and U to the predicted solubilities reported by Denham² reveals the following. Observed Pu concentrations for the reducing RRII samples ranged from 7E-11 to 2E-9 M, which is higher than the predicted values at an E_h of -470 mV for both pure PuO₂ and the co-precipitate phase which ranged from 8E-13 to 3E-11 M. Observed U concentrations for the reducing RRII samples after washing were near 2E-6 M for both sample types (E and F), which is much higher than the predicted values at -470 mV for this condition for both pure UO₃·2H₂O and the co-precipitate phase which ranged from 2E-12 to 5E-09 M (even higher values observed in pre-washed sub-samples).

For the ORII condition, observed Pu concentrations for the filtered leachate samples ranged from 4E-10 to 6E-9 M, which is intermediate in value relative to the predicted values for both pure PuO₂ and the co-precipitate phase which ranged from 7E-12 to 5E-08 M. Observed U concentrations for the ORII leachate samples ranged from 4E-6 to 2E-5 M, which is intermediate in value relative to the predicted values for both pure UO₃·2H₂O and the co-precipitate phase which ranged from 2E-11 to 6E-05 M.

For the ORIII condition, observed Pu concentrations for the filtered leachate samples ranged from 6E-9 to 1E-8 M, which is intermediate in value relative to the predicted values for both pure PuO₂ and the co-precipitate phase which ranged from 1E-13 to 8E-08 M. Observed U concentrations for the ORIII leachate samples ranged from 7E-5 to 4E-4 M. These uranium concentrations exceed the highest predicted uranium concentrations of 4E-06 M by one to two orders of magnitude.

In general, the predicted Pu and U concentrations for co-precipitated phases are all lower than were experimentally observed. Thus we conclude that a significant fraction of the Pu and U in the Tank 18F residual solids sample used in this testing appears to be pure Pu and U oxide phases and not co-precipitated phases. Plutonium concentrations for both of the oxidizing cases (where higher solubilities were expected) did not exceed the predicted values for the cases where dissolved oxygen is assumed. Uranium concentrations observed for both the RRII and ORIII conditions greatly exceeded the predicted

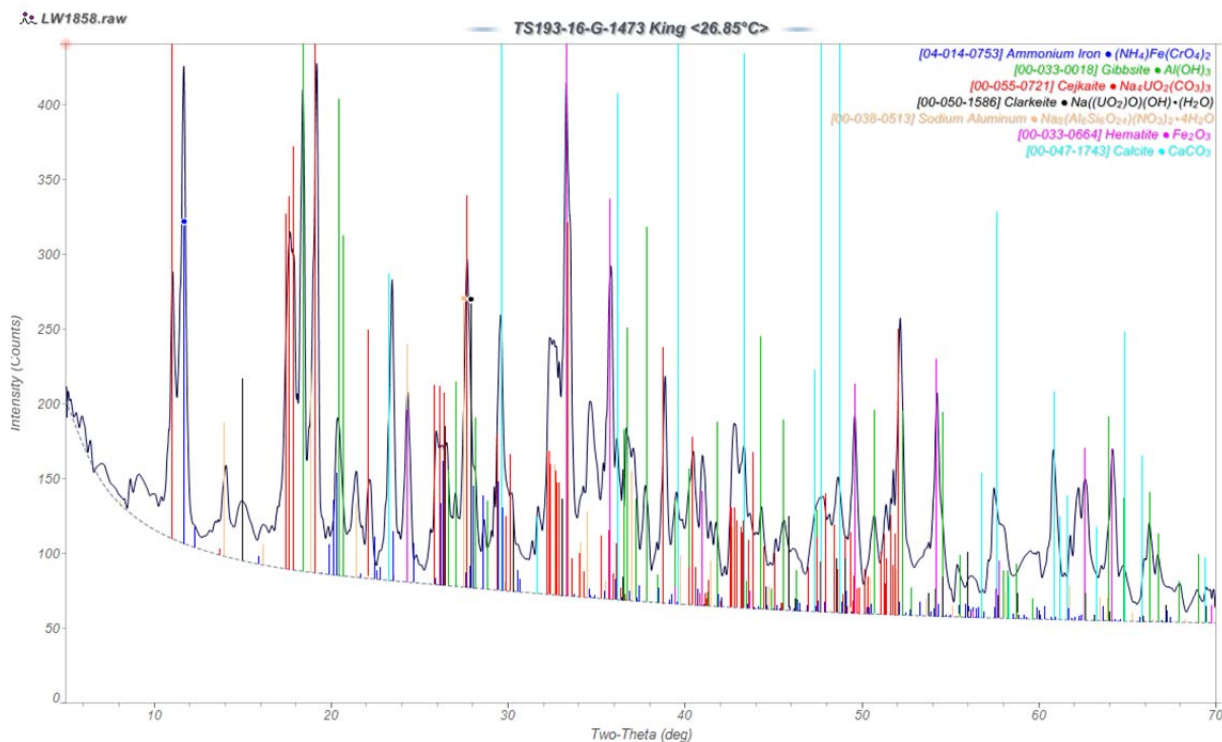


Figure 3-11. XRD Analysis Results for the Original, Archived Tank 18F Residual Solids. Yellow in legend refers to the nitrate-substituted Sodalite phase, $\text{Na}_8(\text{Al}_6\text{Si}_6\text{O}_{24})(\text{NO}_3)_2 \cdot 4\text{H}_2\text{O}$ [00-038-0513].

values, indicating that the uranium speciation in the Tank 18F residuals may be dominated by a more soluble phase than $\text{UO}_3 \cdot 2\text{H}_2\text{O}$. Significant uranium solubility is typically observed in tank sludge wash solutions and a commonly observed uranium crystalline sludge phase is Clarkeite, $\text{Na}((\text{UO}_2)\text{O})(\text{OH}) \cdot \text{H}_2\text{O}$.¹⁰ Sodium diuranate, $\text{Na}_2\text{U}_2\text{O}_7 \cdot 6\text{H}_2\text{O}$, has also been observed in sludge samples.¹¹ The Tank 18F residual sample used for testing included both the Clarkeite uranium phase and a uranium carbonate phase, Cejkaite, $\text{Na}_4\text{UO}_2(\text{CO}_3)_3$ (Figure 3-11), not previously observed in other tank waste samples (also observed in the XRD of an earlier Tank 18F floor sample XRD¹²). Carbonate phases such as this would be expected to be somewhat soluble relative to typical oxide phases.

Technetium and neptunium predicted solubilities as reported by Denham² are provided in Table 3-6. Dramatic shifts in technetium solubility were predicted as the system shifts from reducing to oxidizing conditions due to speciation changes from hydrated TcO_2 to soluble oxidized species such as TcO_4^- . Likewise, neptunium solubility was predicted to increase significantly due to speciation changes from the hydrated NpO_2 phase to the Np(V) species, $\text{NpO}_2(\text{OH})$. As discussed previously steady state technetium concentrations were not observed during Tank 18F residual leach testing over a time period of ~2 months. Consequently, the leachate concentrations of the actual tank pore water also may not reach steady-state depending upon the pore water flow rate through the system. Under reducing conditions (RRII), observed technetium concentrations were below detectable limits (<6E-10 M) and the detection limit was intermediate between the predicted solubilities for pure phase $\text{TcO}_2 \cdot 1.6 \text{H}_2\text{O}$ and the co-precipitate phase which ranged from 1E-14 to 1E-08 M. Technetium concentrations as high as 1E-8 M were observed for the ORII and ORIII conditions (samples A, B, and C) and the data trends indicated that equilibrium and saturation had not been achieved. No solubility limit was reported by Denham² for technetium under

oxidizing conditions, due to the high solubilities of oxidized forms of technetium such as TcO_4^- . Under reducing conditions (RRII), observed neptunium concentrations were below detectable limits ($<2E-10$ M) and the detection limit was intermediate between the predicted solubilities for pure phase NpO_2 and the co-precipitate phase which ranged from $5E-15$ to $1E-09$ M. For the ORII condition, neptunium concentrations were near ($3E-10$ M) or below detection limits ($<2E-10$ M), and these values are intermediate between the predicted solubilities for pure phase NpO_2 and the co-precipitate phase which ranged from $4E-14$ to $7E-07$ M. For the ORIII condition, neptunium concentrations ranged from $1E-09$ to $4E-09$ M, which is intermediate between the predicted solubilities for pure phase NpO_2 and the co-precipitate phase which ranged from $9E-16$ to $5E-05$ M. In general, the predicted Tc and Np concentrations for co-precipitated phases are all lower than were experimentally observed. Thus we conclude that a significant fraction of the Tc and Np in the Tank 18F residual solids used in this testing appears to be pure Tc and Np oxide phases and not co-precipitated phases. Tc and Np concentrations for both of the oxidizing cases (where higher solubilities were expected) did not exceed the predicted values for the cases where dissolved oxygen is assumed.

Table 3-6. Predicted Solubilities of Assumed Tc and Np Phases.

Condition	Initial Phase	E_h (mV)	Tc (M)	Np (M)
RRII ^a	$TcO_2 \cdot 1.6 H_2O$ or NpO_2 (am, hyd) ^d	-470	$1E-08$	$1E-09$
RRII ^c	Maghemite co-precipitate	-470	$1E-14$	$5E-15$
ORII ^a	no Tc solubility controlling phase; NpO_2 (am, hyd) ^d	+240	no limit	$3E-07$
ORII ^b	$NpO_2(OH)$ (am, aged) ^d	+560	---	$7E-07$
ORII ^c	Maghemite co-precipitate	+240	$1E-13$	$4E-14$
ORIII ^a	no Tc solubility controlling phase; NpO_2 (am, hyd) ^d	+290	no limit	$2E-06$
ORIII ^b	$NpO_2(OH)$ (am, aged) ^d	+680	---	$5E-05$
ORIII ^c	Maghemite co-precipitate	+290	$2E-15$	$9E-16$

^a from Table 11 of SRNL-STI-2012-00404²; E_h values represent more realistic, non-equilibrium conditions with dissolved oxygen

^b from Table 12 of SRNL-STI-2012-00404²; E_h values represent equilibrium conditions with dissolved oxygen

^c from Table 14 of SRNL-STI-2012-00404²; represents apparent solubility based on primary iron phase solubility and Fe:Tc:Np ratio

^d solubility based on hydrous (hyd), aged, and amorphous (am) neptunium oxide and oxyhydroxide phases

In addition to the Pu, U, Tc, and Np analyses discussed above, other analyses were conducted as specified in the TTQAP. X-ray diffraction analysis was conducted for the original Tank 18F residual solids as well as one oxidizing and one reducing leachate sample. Diffractograms are provided in Figures 3-11 through 3-13. The original sample was observed to contain multiple phases, making phase identification challenging (Figure 3-11). Uranium phases observed included Clarkeite and Cejkaite, as discussed above. Commonly observed iron and aluminum sludge phases, Hematite and Gibbsite were also present. The nitrate-substituted sodalite phase, $Na_8(Al_6Si_6O_{24})(NO_3)_2 \cdot 4H_2O$, was also present in the sample. This aluminosilicate phase is presumably present due the transfer of Tank 19F waste to Tank 18F.¹³ Tank 19F contained zeolite Cs ion exchange media. Sodalite was also observed in the XRD of Tank 19F solids.¹¹ Other phases observed in original Tank 18F sample included calcite ($CaCO_3$) and the Fe:Cr phase, $(NH_4)Fe(CrO_4)_2$, neither of which are commonly observed tank waste phases. X-ray diffraction analysis was reported previously for this Tank 18F sample and similar results were reported.¹² Differences between the scans included no observance of Hematite or Cejkaite and the observation of a previously unobserved uranium phase, $UO_2HF_3 \cdot 2H_2O$ in the earlier analysis. After leach testing, the XRD scan of the ORIII-C sample indicated that no crystalline uranium phases remained. The dominant Calcite peak in

the scan is a result of the addition of calcium carbonate reagent to the sample. An additional commonly-observed, $\text{Al}(\text{OH})_3$ phase, Bayerite, was also observed. The XRD scan of the RRII-E sample after leach testing was very similar to the scan for the ORIII-C sample except that the Fe:Cr phase was not observed for the reducing sample.

Particle size analysis results are provided in Figures 3-14 through 3-18 for the original Tank 18 residual solids, the ORIII-C post-leach solids, the RRII-E post-leach solids, and the FeS and CaCO_3 reagents. All particle size distributions are plotted on a volume basis. All samples were analyzed for PSD suspended in pore water simulants (ORIII simulant for sample C and calcium carbonate reagent; RRII simulant for the remainder). The FeS reagent (Figure 3-17) had a mean particle diameter of 38 μm and particle range from <10 μm to approximately 200 μm . The CaCO_3 reagent (Figure 3-18) had a mean particle diameter of 35 μm and a diameter range from <10 μm to approximately 100 μm . FeS and CaCO_3 were added to the RRII-E sample, while only CaCO_3 was added to the ORIII-C sample. The mean particle diameter for the original Tank 18 residual solids (Figure 3-14) was 112 μm and the diameter ranged from <10 μm to approximately 700 μm with a monomodal distribution and a peak near 200 μm . This particle size is much larger than typical tank waste samples, which have average particle diameters <10 μm .¹⁴ The mean particle diameter for the ORIII-C sample (Figure 3-15) was much smaller than the original sample, but still large relative to typical sludge with a mean diameter of 10 μm and a diameter range from <1 μm to approximately 100 μm with a bimodal distribution. The broad peak near 25 μm may be associated with the CaCO_3 reagent. The mean particle diameter for the RRII-E sample (Figure 3-16) was much smaller but still large relative to typical sludge with a mean diameter of 8 μm and a diameter range from <1 μm to approximately 35 μm .

Additional analysis was conducted on the ORII-B and RRII-E leachate sub-samples collected during test week 7 for cesium, strontium, technetium (radiochemical analysis), and oxalate (see Table 3-7). Cs-137 was observed in both samples at concentrations ranging from 7E-10 to 4E-09 M. Sr-90 was observed in both leachate samples at concentrations approaching 2E-11 M. Measurable technetium was only observed for the ORII-B sample, as was the case for the ICP-MS analysis (Table 3-1). Surprisingly, the detection limit achieved by beta scintillation counting for the RRII-E sample was not as low as was achieved by ICP-MS. No measurable oxalate was observed in either leachate sample.

Table 3-7. Additional Analysis Conducted on Week 7 Sub-samples.

	Cs-137 (M)	Sr-90 (M)	Tc-99 (M)	Oxalate (M)
ORII-B	4.0E-09	1.7E-11	1.8E-08	<1.3E-04
RRII-E	7.3E-10	1.6E-11	<2.7E-9	<1.3E-04

Americium analysis was conducted for the leachate samples and one control sample collected during week 3 and the results are provided in Table 3-8. Americium was observed at a low level in the control sample (2E-12 M), and most of the leachate samples contained americium at concentrations near that observed for the control. The ORIII-C sample contained significantly higher Am than all other samples (3E-11 M).

Analysis results for the simulant wash solutions from leach test samples ORII-A and ORIII-C are provided in Table 3-9. The appropriate simulants were used to wash the samples (ORII simulant for sample A and ORIII simulant for sample C). Plutonium, uranium, neptunium, and technetium concentrations in the ORII-A wash were equal to or greater than the highest metal concentrations observed for any leach test sample. Plutonium, uranium, and neptunium concentrations observed for the ORIII-C sample were much higher than was observed for any leachate sample.

Table 3-8. Americium Data for Week 3 Sub-samples.

Sample	Am-241 (M)
ORII-A	9.4E-13
ORII-B	3.3E-12
ORII-C	3.0E-11
ORIII-D	8.2E-13
ORIII-E	2.4E-12
RRII-F	2.1E-12
B Control	1.9E-12

The plutonium concentrations in the ORIII-C wash exceeded the predicted concentrations and the uranium and neptunium levels greatly exceeded the predicted concentrations (Tables 3-4 and 3-6). These results confirm that concentrations significantly exceeding those observed in the leachate testing can be achieved during initial liquid contact. The result may also indicate that a fraction of the radionuclides is more soluble than the remainder. Based on these concentrations and the known wash decant volumes, the metal losses for each sample were calculated and are provided in Table 3-10. Mass losses for Pu, Np, and Tc were $\leq 6.5\%$ for both samples. However, calculated uranium losses for ORIII-C were very high and significantly exceeded the total mass believed to be present in the sample. This result indicates that uranium results for the ORIII-C sample and probably for the ORIII-D sample were compromised by the dissolution of uranium from the sample during washing. These results are consistent with the observation of no uranium phases in the XRD of the post-leach ORIII-C sample (Figure 3-12). The observation of high metal solubilities is not surprising given the Tank 18 processing history and the likely formation of carbonate species as discussed in an earlier report.¹⁵ As discussed above, a crystalline uranium carbonate phase was observed for the Tank 18F sample. In addition, the formation of plutonium and neptunium carbonate phases is also likely.

Table 3-9. ORII-A and ORIII-C Wash Sample Analysis Results.

	Pu (M)	U (M)	Np (M)	Tc (M)	Oxalate (M)
ORII-A	4.0E-08	3.2E-04	1.3E-09	1.0E-08	1.2E-03
ORIII-C	3.0E-07	4.6E-03	2.9E-08	9.4E-09	1.2E-03

Table 3-10. Metal Losses to Tank 18F Residual Washes Prior to Leach Testing Calculated Based on Wash Analysis.

	Pu Loss (%)	U Loss (%)	Np Loss (%)	Tc Loss (%)
ORII-A	0.3	12.3	0.2	6.2
ORIII-C	2.6	174	5.3	5.9

Digestion of the original Tank 18 residual solids and leachate samples ORIII-C and RRII-E was conducted and the digestion products were analyzed. The elemental composition (wt. %) of the samples is provided in Table 3-11. Direct comparison of the results is difficult without normalizing the data to the value for a metal such as Al (assuming minimal Al dissolution although the solution pH was near 11). The normalized results are provided in Table 3-12. Comparison of the normalized results reveals that the Tank 18 residual composition in each of the samples is similar. Elevated Ca (sample C) and Ca and Fe (sample E) levels resulting from the addition of $\text{Ca}(\text{CO})_3$ and FeS reagent are apparent in the table. In addition, no detectable uranium was observed for the ORIII-C residual sample, which is consistent with the high uranium concentrations observed for the wash sample in Table 3-9. The weight percent values for Pu, Np, and Tc in the ORII-A and ORIII-C samples in Table 3-12 are all $\geq 80\%$ of the values observed for the original Tank 18 F sample.

Scanning Electron Microscopy (SEM) results for the original Tank 18 residual solids, the ORIII-C post-leach solids, and the RRII-E post-leach solids are provided in the Appendix. Results were as expected for each sample. Results for the original Tank 18F residual sample are provided in Figures A-1 through A-5. Bulk observed metals included Al, Ca, Fe, Na, Mn, Mg, Si, and U. The composition of some localized spots within the sample indicated high levels of uranium (Figure A-4). Results for the ORIII-C post-leach solids are provided in Figures A-6 through A-10. Elements observed during analysis of the bulk sample included the above-mentioned elements excluding uranium. Uranium was observed at low levels in some localized analysis. Calcium was present at higher levels in this sample than was observed in the original sample due to the addition of calcium carbonate reagent. Localized regions of the sample were identified which were more concentrated in aluminum (Figure A-9) and calcium (Figure A-10). SEM results for the RRII-E post-leach solids are provided in Figures A-11 through A-14. Elements observed during analysis of the bulk sample included all of the above-mentioned elements observed for the original sample as well as sulfur, resulting from the addition of FeS reagent to this sample. Calcium levels were high relative to the original sample due to the addition of calcium carbonate reagent. Localized regions were also observed with high levels of iron and sulfur, due to the addition of FeS reagent. Plutonium was not observed in any samples due to the low amount of plutonium present.

Table 3-11. Elemental Composition of Original Tank 18F Residual Solids and ORIII-C and RRII-E Leachate Samples at Test Conclusion.

Element	Wt. %		
	Tank 18F	ORIII-C	RRII-E
Al	10.3	9.3	7.3
Ca	3.3	18.2	15.9
Fe	9.3	7.5	13.9
Mg	4.0	2.8	2.2
Mn	1.0	0.8	0.6
Si	2.2	1.9	1.6
U	6.3	<0.4	3.5
Tc-99	2.2E-04	1.7E-04	1.3E-04
Np-237	7.9E-04	6.0E-04	4.6E-04
Pu-239	2.2E-02	1.6E-02	1.3E-02
Pu-240	1.4E-03	1.1E-03	7.8E-04

Table 3-12. Elemental Weight Percentages Normalized to Aluminum for Original Tank 18F Residual Solids and ORIII-C and RRII-E Leachate Samples at Test Conclusion.

Element	Wt. %		
	Tank 18F	ORIII-C	RRII-E
Al	1.0	1.0	1.0
Ca	0.3	2.0	2.2
Fe	0.9	0.8	1.9
Mg	0.4	0.3	0.3
Mn	0.1	0.1	0.1
Si	0.2	0.2	0.2
U	0.6	<0.04	0.5
Tc-99	2.1E-05	1.8E-05	1.7E-05
Np-237	7.6E-05	6.4E-05	6.3E-05
Pu-239	2.1E-03	1.7E-03	1.7E-03
Pu-240	1.3E-04	1.2E-04	1.1E-04

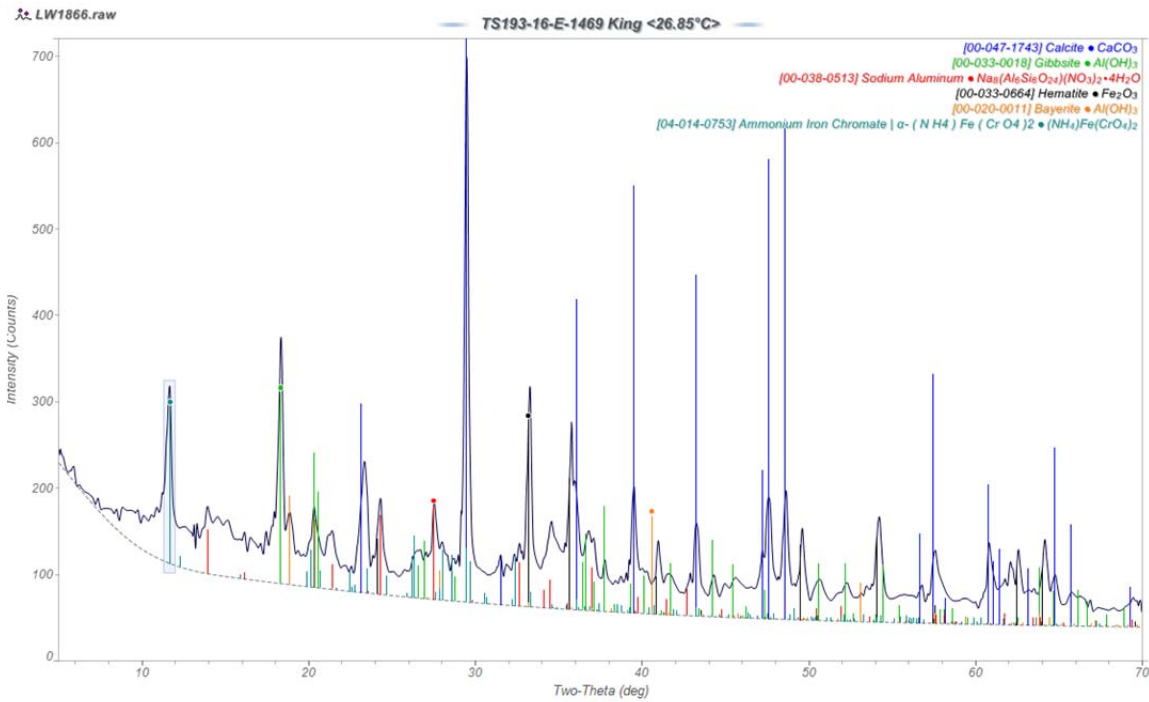


Figure 3-12. XRD Analysis Results for the Tank 18F Residual Solids ORIII-C Leachate Sample at Test Conclusion. Yellow in legend refers to Bayerite, Al(OH)₃ [00-020-0011].

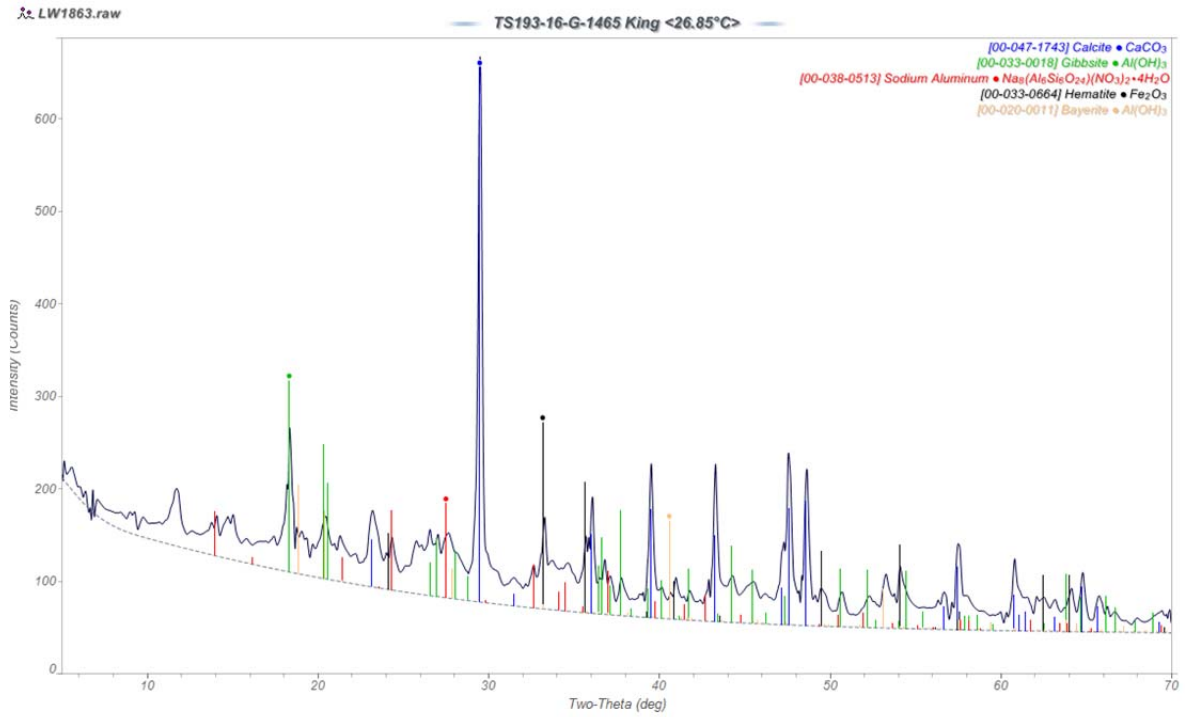


Figure 3-13. XRD Analysis Results for the Tank 18F Residual Solids RRII-E Leachate Sample at Test Conclusion. Yellow in legend refers to Bayerite, Al(OH)₃ [00-020-0011].

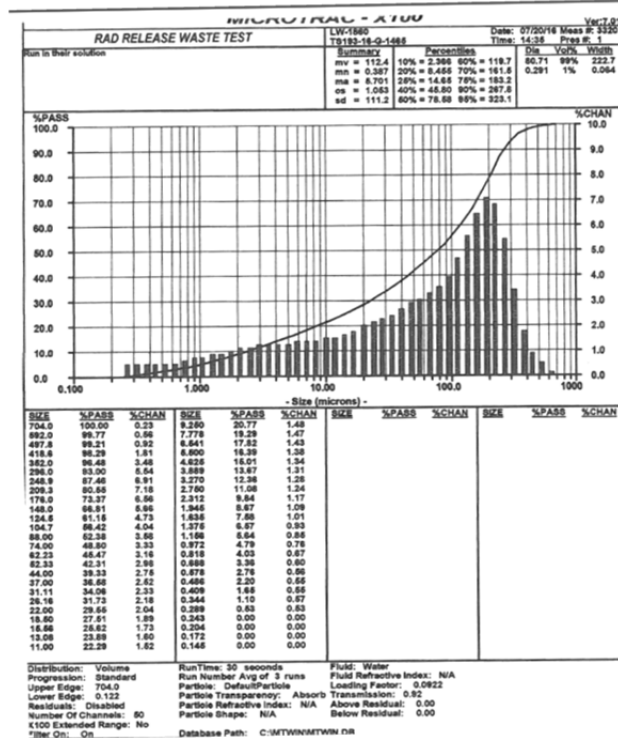


Figure 3-14. Volume-Based Particle Size Distribution for the Original Tank 18 Residual Solids in RRII Simulant.

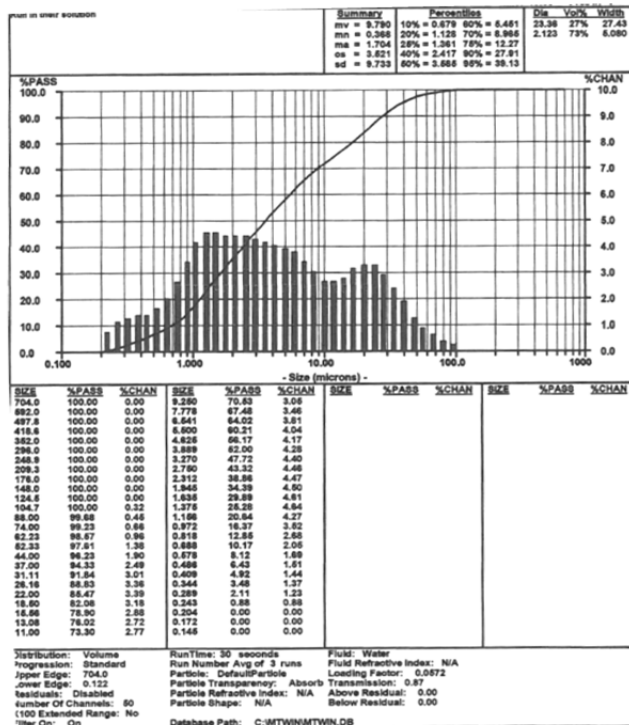


Figure 3-15. Volume-Based Particle Size Distribution for the ORIII-C Leachate Sample at Test Conclusion.

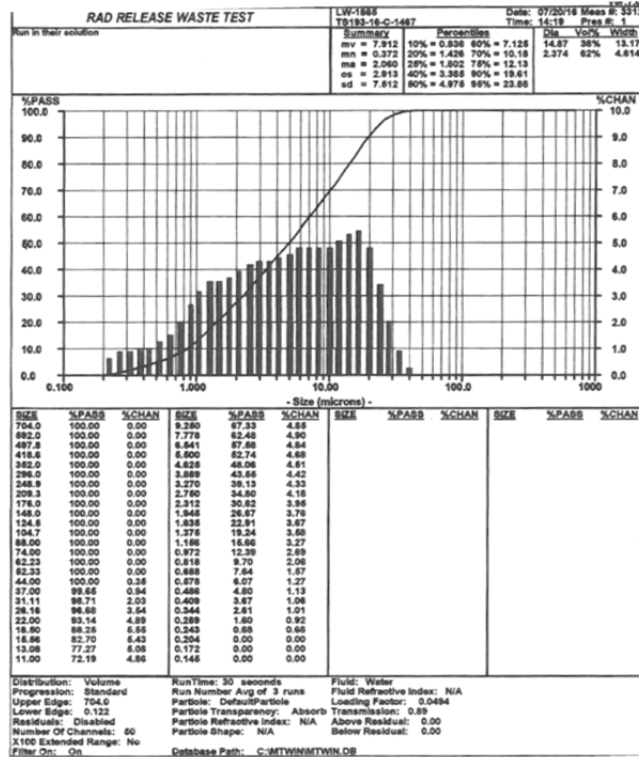


Figure 3-16. Volume-Based Particle Size Distribution for the RRII-E Leachate Sample at Test Conclusion.

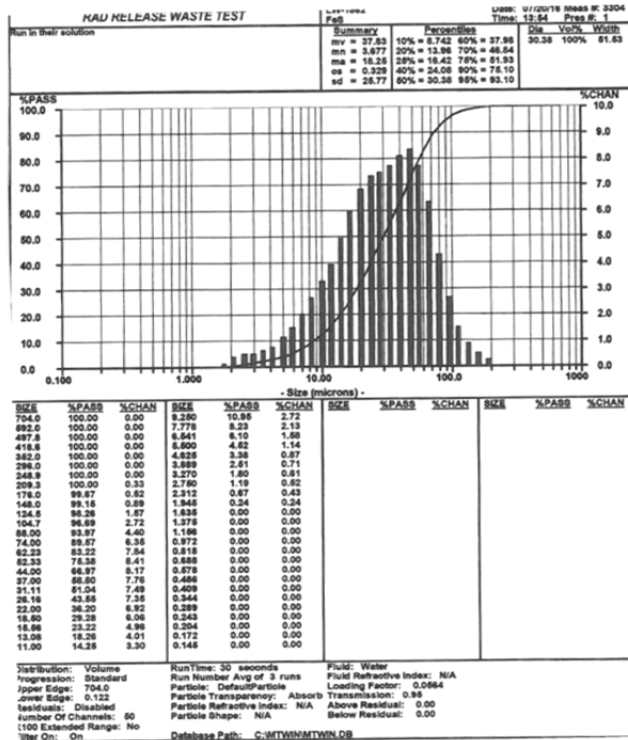


Figure 3-17. Volume-Based Particle Size Distribution for the FeS Reagent in RRII Simulant.

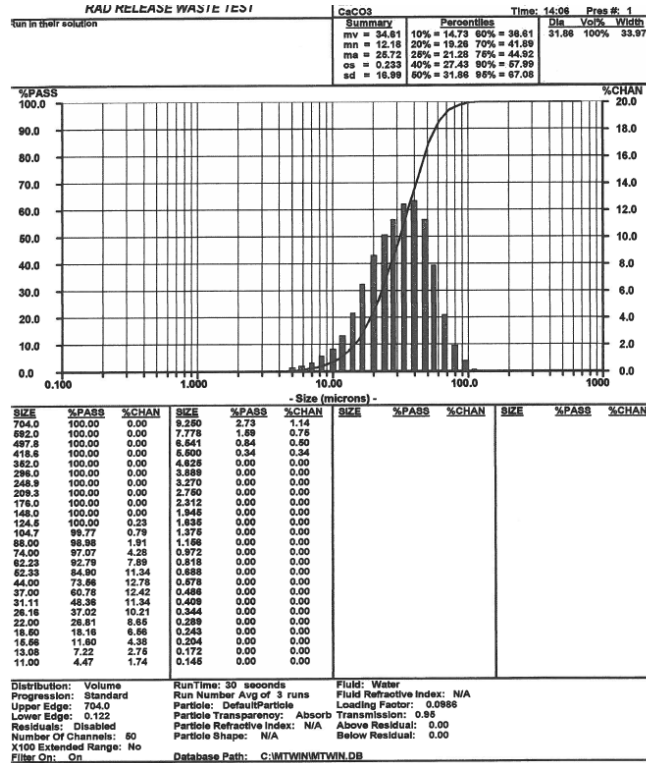


Figure 3-18. Volume-Based Particle Size Distribution for the CaCO₃ Reagent in ORIII Simulant.

4.0 Conclusions

Leaching studies were completed for actual SRS Tank 18F residual solids using customized test equipment and a sub-sampling system and sample handling methodology designed to minimize or eliminate sample contamination from the SRNL shielded cells test facility. Very low leachate metal concentrations (near analytical detection limits in some cases) were analyzed along with blank samples to confirm the suitability of the testing approach. Results indicate that the concentrations of plutonium, technetium, and neptunium in washed samples were below the maximum predicted concentrations utilized for PA modeling. Trends in the technetium data indicate that equilibrium and saturation were not achieved during the 2-month testing period. Observed uranium concentrations exceeded the maximum predicted concentrations utilized for the PA, presumably due to the differences between the actual and assumed chemical speciation. After test conclusion it was discovered that significant losses of uranium to the wash solutions occurred for oxidizing samples and that the concentrations of uranium, plutonium and neptunium were higher in the wash solutions than in any leachate samples analyzed. The metal concentrations in the wash samples were greater than the maximum predicted concentrations assumed and utilized for PA modeling. This was an unexpected result and is presumably associated with the fact that more soluble chemical forms of these metals are present. Due to the uranium losses to the wash and the apparent near depletion of uranium from the samples, the uranium concentrations reported for the ORIII samples are not believed to represent solubility limits. Despite the discovery of high metal concentrations in the wash solutions the measured leachate concentrations are believed to be representative of the maximum concentrations that might be observed during the major portion of the tank aging time periods of interest. In addition, it should be emphasized that during tank aging, more gradual transitions from reducing to oxidizing conditions are expected which should help to minimize the occurrence of pulses of more concentrated metal release that might otherwise be expected based on the high concentrations in the wash solutions.

5.0 Recommendations, Path Forward, and Future Work

Based on the results, it is believed that the current testing methods and equipment were successfully utilized to evaluate the leaching properties of Tank 18F residual solids. It is recommended that similar testing be conducted on other archived tank residual samples to determine the leaching characteristic of residual solids exposed to oxalic acid cleaning. In future testing, additional emphasis should be placed on early analysis of the wash solutions to evaluate metal losses to the wash.

6.0 References

1. "Performance Assessment for the H-Area Tank Farm at the Savannah River Site", SRR-CWDA-2010-00128, Rev. 1, November 2012.
2. M. E. Denham and M. R. Millings, "Evolution of Chemical Conditions and Estimated Solubility Controls on Radionuclides in the Residual Waste Layer during Post-Closure Aging of High-Level Waste Tanks", SRNL-STI-2012-00404, August 2012.
3. K. H. Rosenberger, "Savannah River Site Liquid Waste Facilities Performance Assessment Maintenance Program FY2015 Implementation Plan", SRR-CWDA-2014-00108, January 2015.
4. Technical Task Request, "Tank Waste Testing to Evaluate Residual Waste Solubility Assumptions used in the Tank Farm PAs", HLE-TTR-2013-002, Rev. 3, September 2015.
5. D. H. Miller, K. A. Roberts, K. M. L. Taylor-Pashow, and D. T. Hobbs, "Determining the Release of Radionuclides from Tank Waste Residual Solids", SRNL-STI-2014-00456, September 2014.
6. W. D. King and D. T. Hobbs, "Determining the Release of Radionuclides from Tank Waste Residual Solids: FY2015 Report", SRNL-STI-2015-00446, September 2015.
7. W. D. King, D. T. Hobbs, M. S. Hay, "Task Technical and Quality Assurance Plan for Determining the Radionuclide Release from Tank Waste Residual Solids", SRNL-RP-2013-00203, Rev. 3, October 2015.
8. L. N. Oji, D. Diprete, and C. J. Coleman, "Characterization of Additional Tank 18F Samples", SRNL-STI-2010-00386, September 2010.
9. W. D. King, "Radionuclide Release", Experiment A2341-00117-04, SRNL E-Notebook (Production), Savannah River National Laboratory, Aiken, SC 29808 (June 2015).
10. W. D. King, T. B. Edwards, D. T. Hobbs, W. R. Wilmarth, "Solubility of Uranium and Plutonium in Alkaline Savannah River Site High Level Waste Solutions", *Separation Science and Technology*, Vol. 45, pp. 1793–1800 (2010).
11. W. D. King and M. S. Hay, "Alternative Enhanced Chemical Cleaning: Basic Studies Results FY09", SRNL-STI-2009-00791, February 2010.
12. M. S. Hay, P. E. O'Rourke, and H. M. Ajo, "Scanning Electron Microscopy and X-Ray Diffraction Analysis of Tank 18 Samples", SRNL-STI-2012-00123, March 2012.
13. J. L. Newman, "Sampling, Analysis, and Characterization Plan to Support HLW Tank 18 Closure", CBU-LTS-2003-00015, Rev. 1, July 2003.
14. D. Click, "Tank 51H-Sludge Batch 4 Particle Size Evaluation and Comparison to Tank 40-Sludge Batch 3", SRNL-ADS-2005-00646, November 2005.
15. D. T. Hobbs, "Form and Aging of Plutonium in Savannah River Site Waste Tank 18", SRNL-STI-2012-00106, February 2012.

Appendix A. SEM Analysis Results.

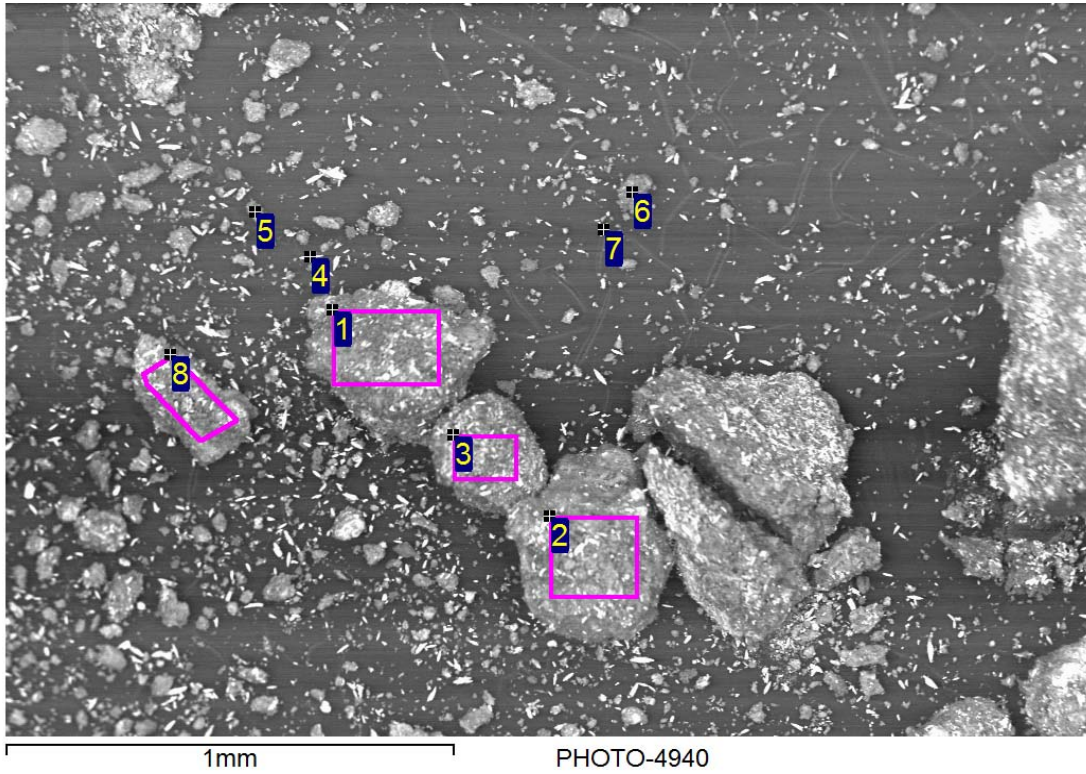


Figure A-1. Low Magnification View of Original Tank 18F Residual.

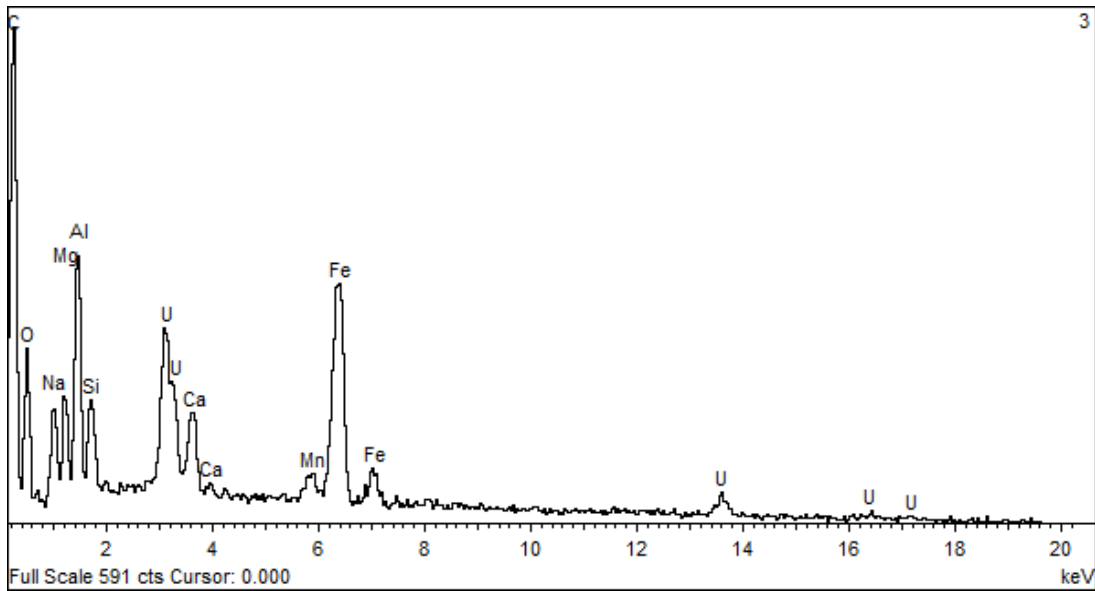


Figure A-2. Bulk Elemental Composition (Spot 3 from Figure A-1) of Original Tank 18F Residual.

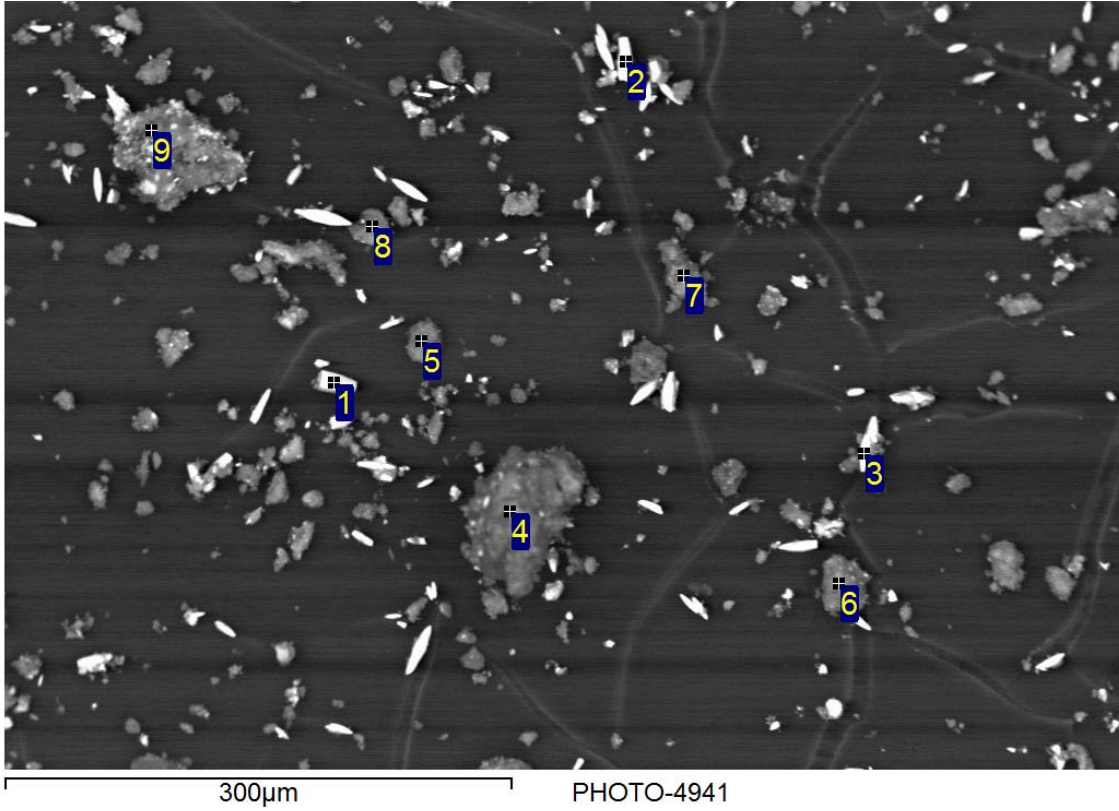


Figure A-3. Higher Magnification View of Original Tank 18F Residual.

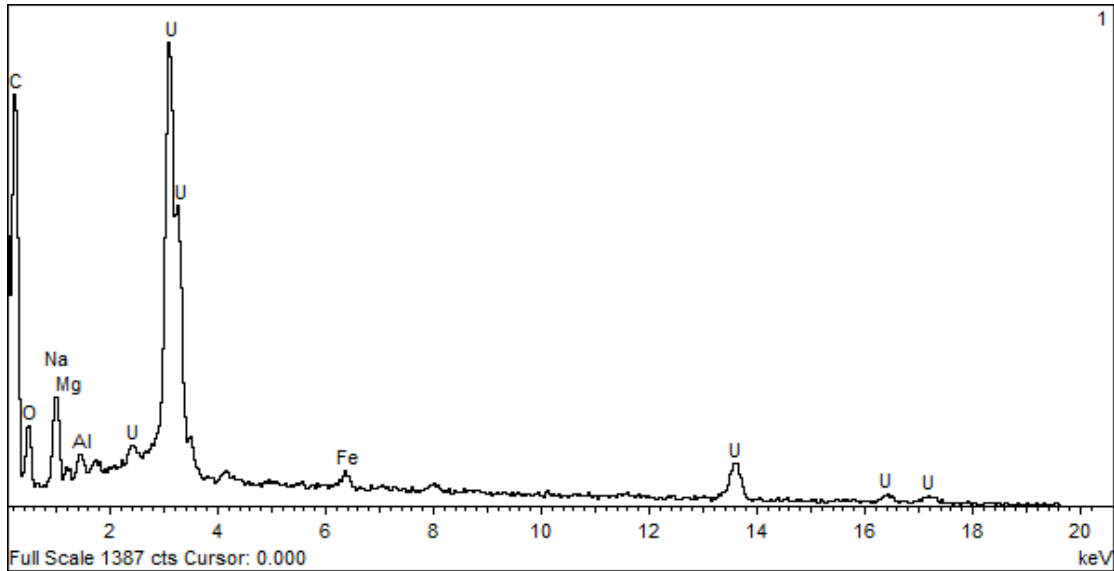


Figure A-4. Elemental Composition (Spot 1 from Figure A-3) of Original Tank 18F Residual.

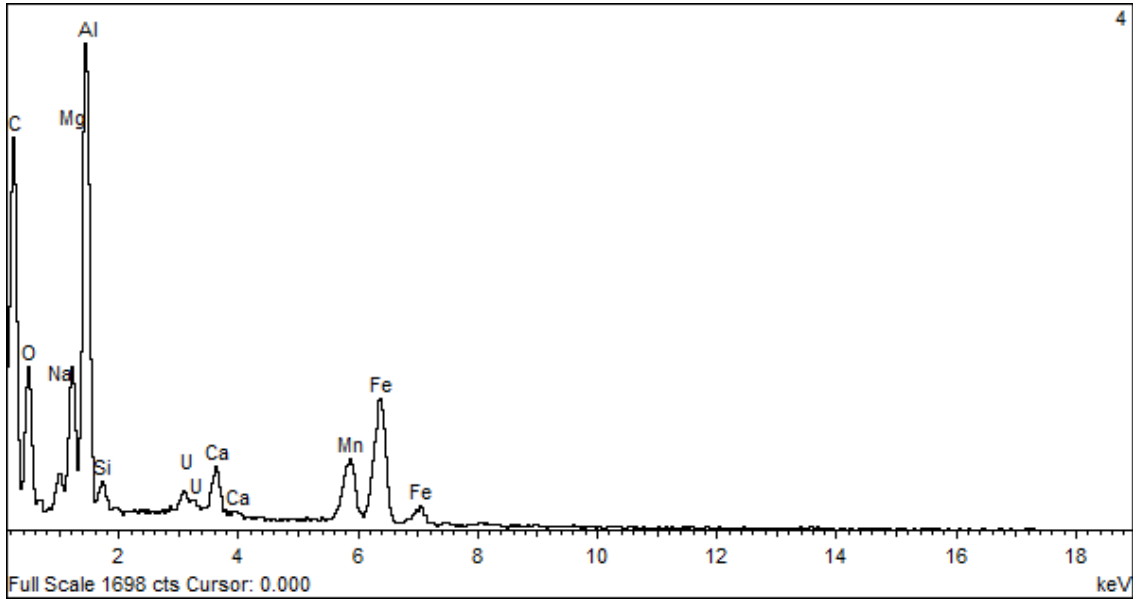


Figure A-5. Elemental Composition (Spot 4 from Figure A-3) of Original Tank 18F Residual.

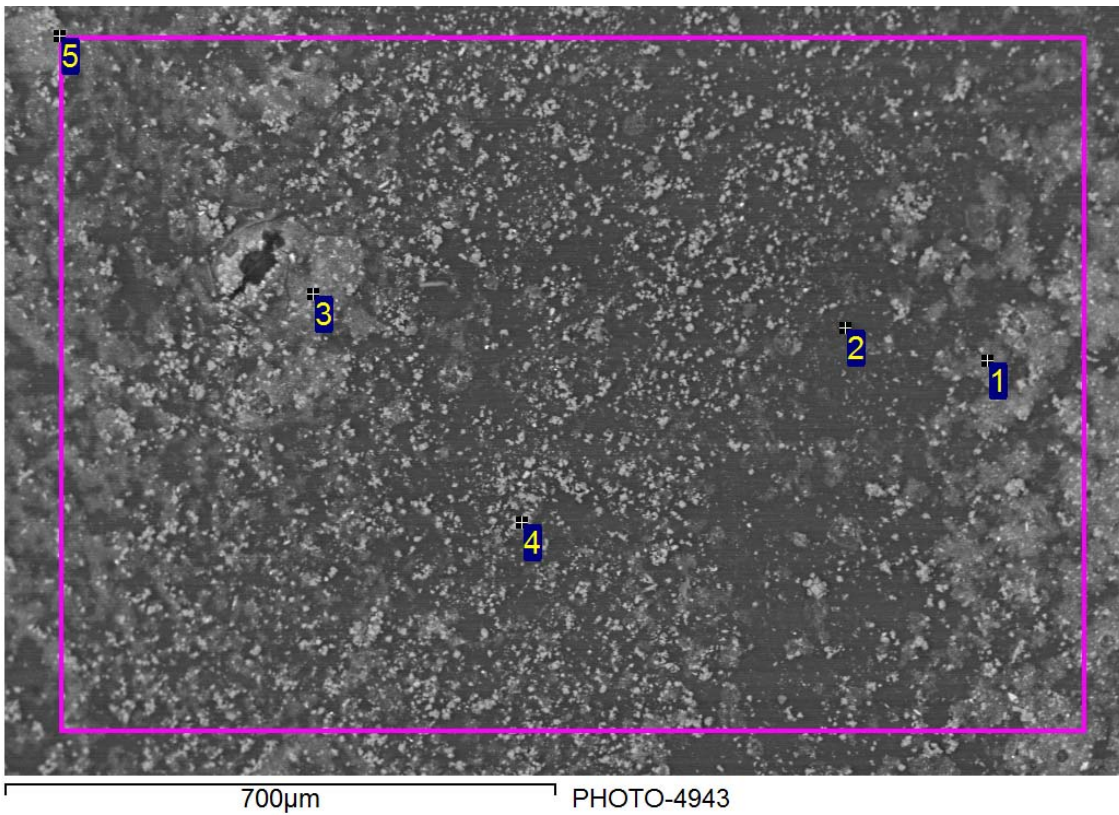


Figure A-6. Low Magnification View of ORIII-C Test Sample.

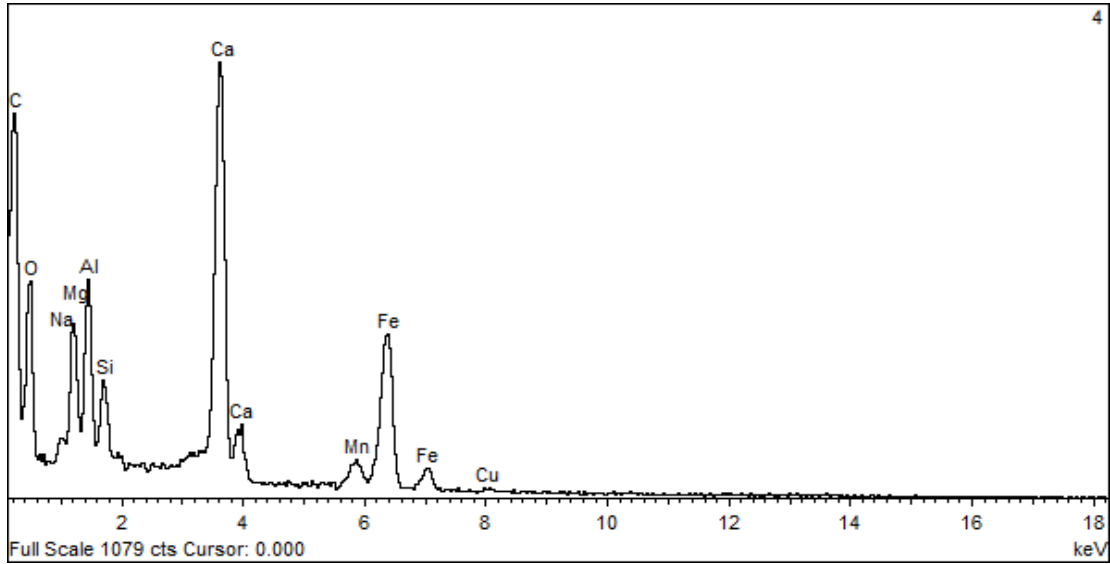


Figure A-7. Bulk Elemental Composition (Spot 4 from Figure A-6) of ORIII-C Test Sample.

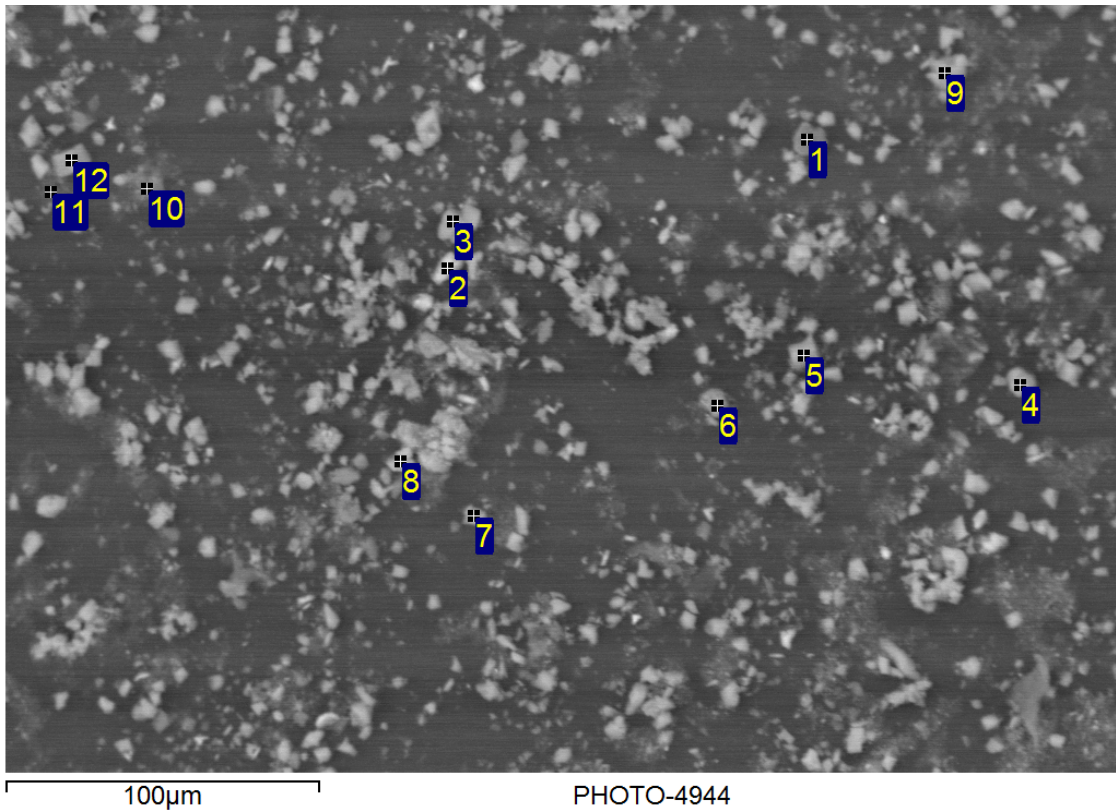


Figure A-8. Higher Magnification View of ORIII-C Test Sample.

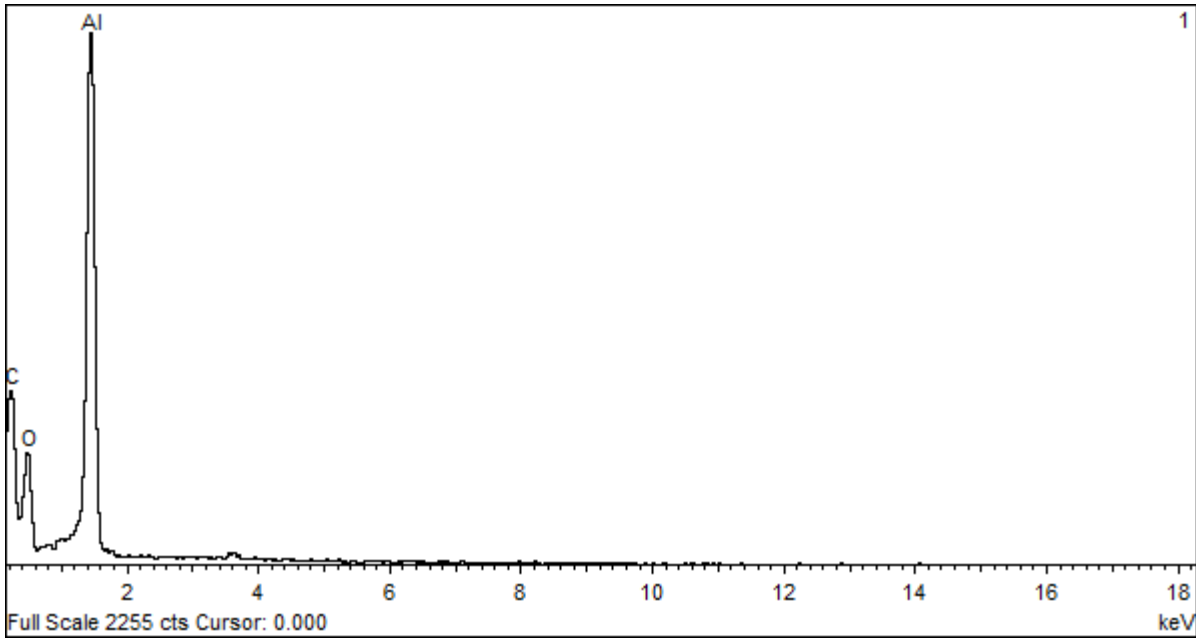


Figure A-9. Elemental Composition (Spot 1 from Figure A-8) for ORIII-C Test Sample.

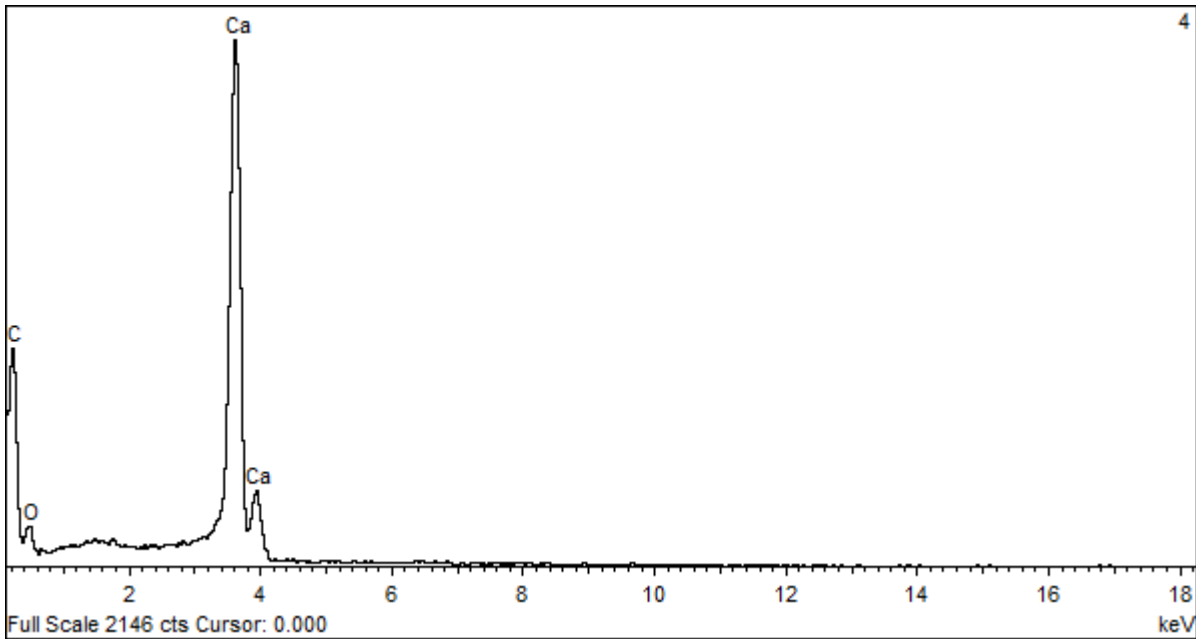


Figure A-10. Elemental Composition (Spot 4 from Figure A-8) for ORIII-C Test Sample.

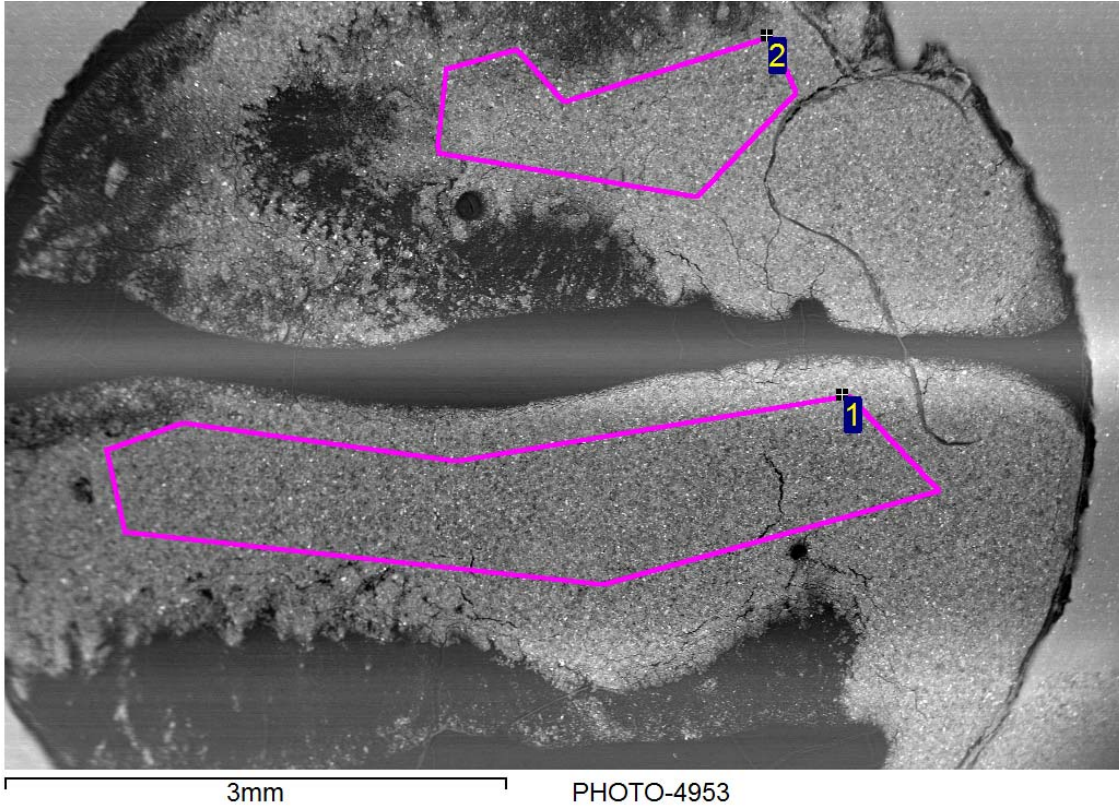


Figure A-11. Low Magnification View of RRII-E Test Sample.

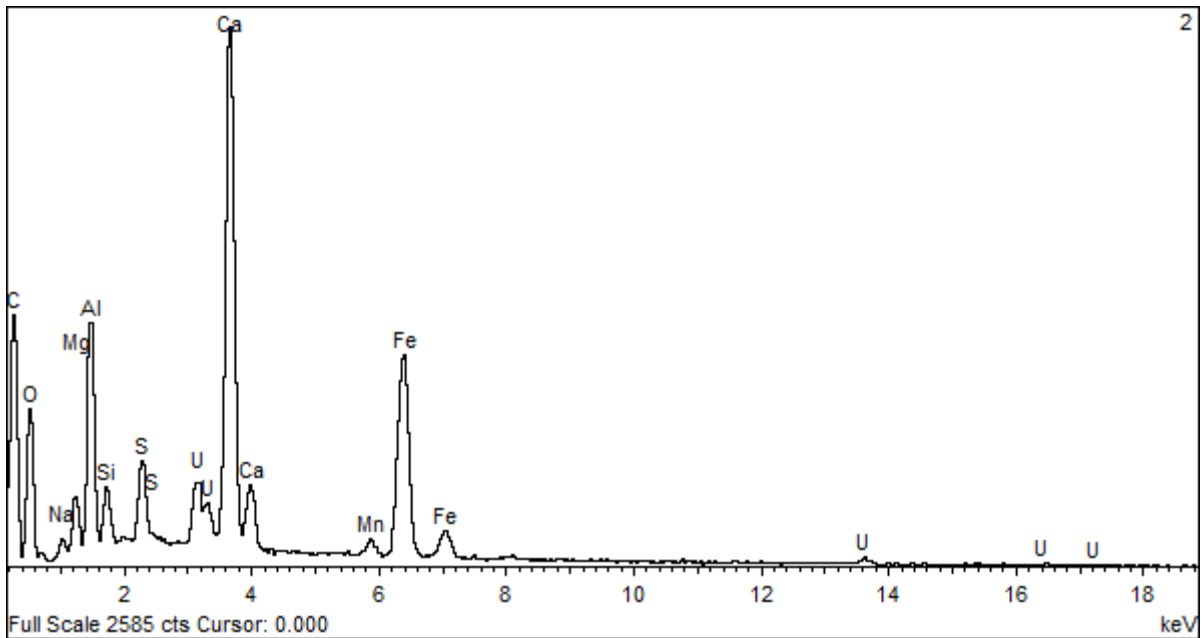


Figure A-12. Bulk Elemental Composition (Spot 2 from Figure A-11) of RRII-E Test Sample.

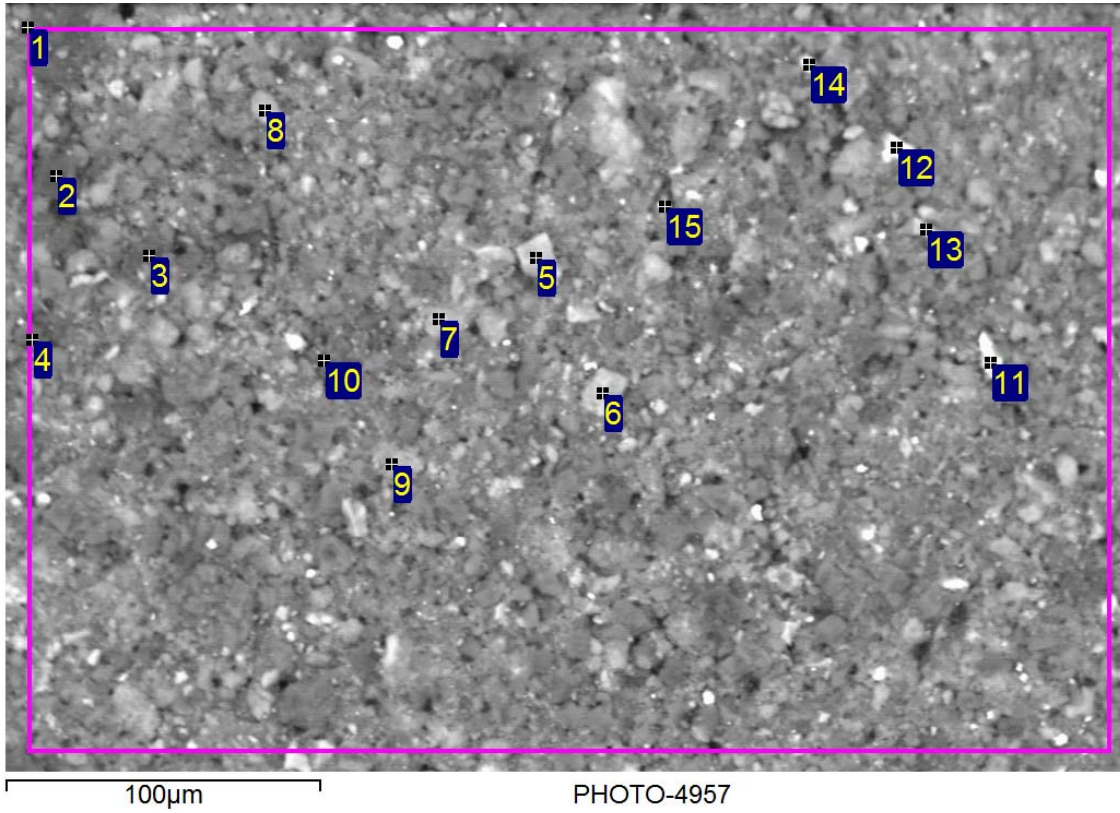


Figure A-13. Higher Magnification View of RRII-E Test Sample.

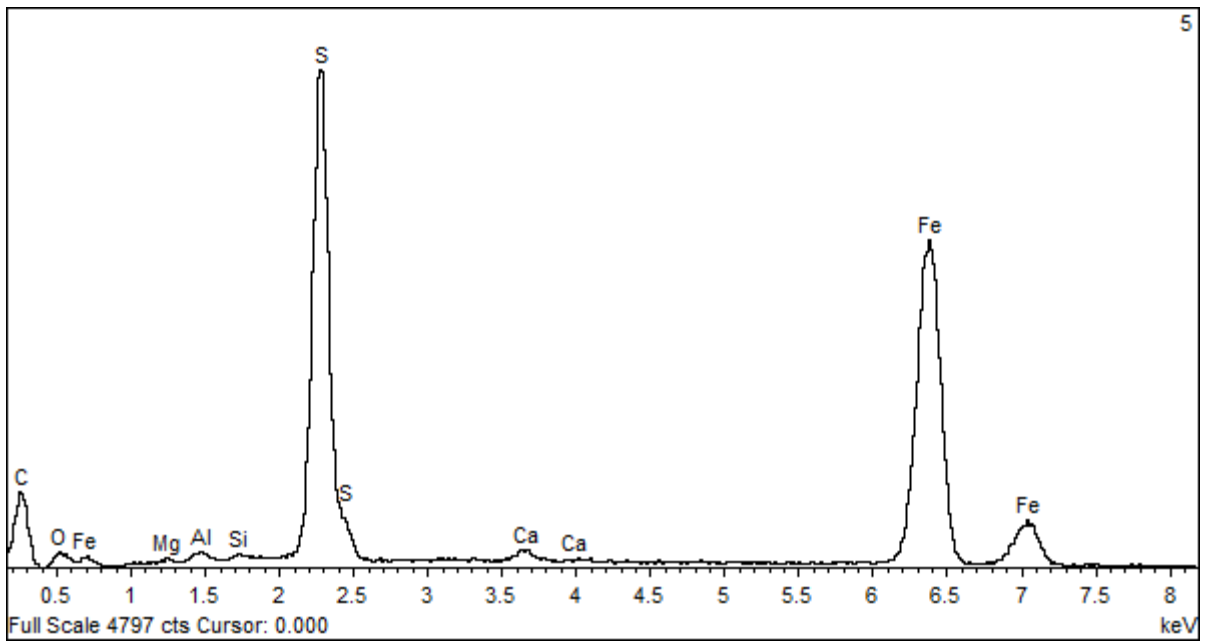


Figure A-14. Elemental Composition (Spot 5 from Figure A-13) for RRII-E Test Sample.

Distribution:

S. A. Thomas, 705-1C
L. B. Romanowski, 705-1C
K. H. Rosenberger, 705-1C
M. K. Layton, 705-1C
K. D. Dixon, 705-1C
T. W. Coffield, 705-1C
J. C. Griffin, 773-A
A. P. Fellingner, 773-42A
T. B. Brown, 773-A
D. H. McGuire, 999-W
S. D. Fink, 773-A
C. C. Herman, 773-A
E. N. Hoffman, 999-W
B. J. Wiedenman, 773-42A
F. M. Pennebaker, 773-42A
W. R. Wilmarth, 773-A
M. E. Stone, 999-W
P. R. Jackson, DOE-SR, 703-46A
J. A. Crenshaw, 703-46A
B. T. Butcher, 773-43A
D. A. Crowley, 773-42A
G. P. Flach, 773-42A
L. L. Hamm, 735-A
R. A. Hiergesell, 773-42A
G. K. Humphries, 730-4B
D. I. Kaplan, 773-42A
D. Li, 773-42A
M. A. Phifer, 773-42A
R. R. Seitz, 773-42A
F. G. Smith, III 773-42A
M. E. Denham, 773-42A
Records Administration (EDWS)